

1    **The 22q11.2 region regulates presynaptic gene-products linked to schizophrenia**

2  
3    Ralda Nehme<sup>1,2 #\*</sup>, Olli Pietiläinen<sup>1,2,##</sup>, Mykyta Artomov<sup>1,3</sup>, Matthew Tegtmeyer<sup>1,2</sup>, Christina  
4    Bell<sup>15</sup>, Andrea Ganna<sup>1</sup>, Tarjinder Singh<sup>1</sup>, Aditi Trehan<sup>1,2</sup>, Vera Valakh<sup>1,2</sup>, John Sherwood<sup>1,2</sup>,  
5    Danielle Manning<sup>1</sup>, Emily Peirent<sup>1,2</sup>, Rhea Malik<sup>2</sup>, Ellen J. Guss<sup>2</sup>, Derek Hawes<sup>1,2</sup>, Amanda  
6    Beccard<sup>1</sup>, Anne M. Bara<sup>1,2</sup>, Dane Z. Hazelbaker<sup>1</sup>, Emanuela Zuccaro<sup>2</sup>, Giulio Genovese<sup>1</sup>,  
7    Alexander A Loboda<sup>1,4</sup>, Anna Neumann<sup>1</sup>, Christina Lilliehook<sup>1</sup>, Outi Kuismin<sup>5,6,7,8</sup>, Eija  
8    Hamalainen<sup>9</sup>, Mitja Kurki<sup>1,5,9</sup>, Christina M. Hultman<sup>10</sup>, Anna K. Kähler<sup>10</sup>, Joao A. Paulo<sup>15</sup>, Jon  
9    Madison<sup>1</sup>, Bruce Cohen<sup>11</sup>, Donna McPhie<sup>11</sup>, Rolf Adolfsson<sup>12</sup>, Roy Perlis<sup>13</sup>, Ricardo  
10   Dolmetsch<sup>14</sup>, Samouil Farhi<sup>1</sup>, Steven McCarroll<sup>1</sup>, Steven Hyman<sup>1,2</sup>, Ben Neale<sup>1</sup>, Lindy E.  
11   Barrett<sup>1,2</sup>, Wade Harper<sup>15</sup>, Aarno Palotie<sup>1,5,16,9,17</sup>, Mark Daly<sup>1,5,15,9,17</sup>, Kevin Eggan<sup>1,2\*</sup>

12  
13    <sup>1</sup> Stanley Center for Psychiatric Research, Broad Institute of Harvard and MIT, Cambridge, MA  
14    02142, USA

15    <sup>2</sup> Department of Stem Cell and Regenerative Biology, and the Harvard Institute for Stem Cell  
16    Biology, Harvard University, Cambridge, MA 02138, USA

17    <sup>3</sup> Analytic and Translational Genetics Unit, Department of Medicine, Massachusetts General  
18    Hospital, Boston, MA, 02114, USA.

19    <sup>4</sup> ITMO University, St. Petersburg, Russia

20    <sup>5</sup> Psychiatric & Neurodevelopmental Genetics Unit, Massachusetts General Hospital, Boston,  
21    MA, 02114, USA

22    <sup>6</sup> PEDEGO Research Unit, University of Oulu, FI-90014, Oulu, Finland

23    <sup>7</sup> Medical Research Center, Oulu University Hospital, University of Oulu, FI-90014, Oulu,  
24    Finland.

25    <sup>8</sup> Department of Clinical Genetics, Oulu University Hospital, 90220, Oulu, Finland.

26    <sup>9</sup> Institute for Molecular Medicine Finland, University of Helsinki, FI-00014, Helsinki, Finland

27    <sup>10</sup> Department of Medical Epidemiology and Biostatistics, Karolinska Institutet, SE-171 77  
28    Stockholm, Sweden

29    <sup>11</sup> McLean Hospital, 115 Mill St., Belmont, MA 02478

30    <sup>12</sup> Umea University, Faculty of Medicine, Department of Clinical Sciences, Psychiatry, 901 85  
31    Umea, Sweden

32    <sup>13</sup> Psychiatry Dept., Massachusetts General Hospital, Boston, MA 02114, USA

33    <sup>14</sup> Novartis Institutes for Biomedical Research, Novartis, Cambridge, MA 02139, USA

34    <sup>15</sup> Department of Cell Biology, Blavatnik Institute of Harvard Medical School, Boston, MA,  
35    USA

36    <sup>16</sup> Institute for Molecular Medicine Finland, University of Helsinki, FI-00014, Helsinki, Finland

37    <sup>17</sup> Department of Neurology, Massachusetts General Hospital, Boston, MA, 02114, USA.

38    <sup>18</sup> BioMarin Pharmaceutical, San Rafael, CA 94901

39    # Contributed equally

40    \* Co-senior authors, and correspondence:

41    [rnehme@broadinstitute.org](mailto:rnehme@broadinstitute.org)

42    [ollip@broadinstitute.org](mailto:ollip@broadinstitute.org)

43    [eggan@mcb.harvard.edu](mailto:eggan@mcb.harvard.edu), [kevin.eggan@bmrn.com](mailto:kevin.eggan@bmrn.com)

48 **Abstract**

49 **To study how the 22q11.2 deletion predisposes to psychiatric disease, we generated induced**  
50 **pluripotent stem cells from deletion carriers and controls, as well as utilized CRISPR/Cas9**  
51 **to introduce the heterozygous deletion into a control cell line. Upon differentiation into**  
52 **neural progenitor cells, we found the deletion acted in trans to alter the abundance of**  
53 **transcripts associated with risk for neurodevelopmental disorders including Autism**  
54 **Spectrum Disorder. In more differentiated excitatory neurons, altered transcripts encoded**  
55 **presynaptic factors and were associated with genetic risk for schizophrenia, including**  
56 **common (per-SNP heritability  $p(\tau_c) = 4.2 \times 10^{-6}$ ) and rare, loss of function variants ( $p =$**   
57  **$1.29 \times 10^{-12}$ ). These findings suggest a potential relationship between cellular states,**  
58 **developmental windows and susceptibility to psychiatric conditions with different ages of**  
59 **onset. To understand how the deletion contributed to these observed changes in gene**  
60 **expression, we developed and applied PPItools, which identifies the minimal protein-**  
61 **protein interaction network that best explains an observed set of gene expression**  
62 **alterations. We found that many of the genes in the 22q11.2 interval interact in**  
63 **presynaptic, proteasome, and JUN/FOS transcriptional pathways that underlie the broader**  
64 **alterations in psychiatric risk gene expression we identified. Our findings suggest that the**  
65 **22q11.2 deletion impacts genes and pathways that may converge with risk loci implicated**  
66 **by psychiatric genetic studies to influence disease manifestation in each deletion carrier.**

67

68

69

70

71 **Introduction**

72 Heterozygous deletions of the 22q11.2 chromosomal interval occur approximately once  
73 in every 4,000 live births<sup>1</sup>. This deletion confers a risk of developing several symptomatically  
74 diverse neuropsychiatric conditions including intellectual disability (ID), Autism Spectrum  
75 Disorder (ASD) and schizophrenia<sup>2-7</sup>. In fact, deletion of 22q11.2 confers the largest effect of  
76 any known genetic risk factor for schizophrenia<sup>8</sup>.

77 Unlike the 22q13.3 deletion syndrome, where risk of mental illness can largely be  
78 explained by reduced function of a single gene (*SHANK3*)<sup>9</sup>, mutations in no one gene within the  
79 22q11.2 deletion can explain the predisposition for psychiatric disease it confers. As a result, the  
80 pathways through which the 22q11.2 deletion contributes to ASD and schizophrenia risk remain  
81 poorly understood. Mouse models have served as an initial in road for identifying genes within  
82 the deletion that function in brain development and behavior. Overall, studies with rodent models  
83 suggest that several genes in the syntenic chromosomal interval including *Dgcr8*, *Ranbp1*, *Rtn4r*,  
84 and *Zdhhc8* have important nervous system functions<sup>10-21</sup>. However, imperfect alignment  
85 between mouse behavioral phenotypes and psychiatric symptoms have left uncertainty  
86 concerning which, or how many of their human orthologs play a role in mental illness.

87 More recent studies now suggest that the genetic background of 22q11.2 deletion carriers  
88 contributes meaningfully to their likelihood of developing one psychiatric condition or another.  
89 For instance, deletion carriers that also harbor an additional copy number variant (CNV)  
90 elsewhere in the genome displayed a higher risk of developing schizophrenia<sup>22</sup>. Additionally,  
91 analysis of polygenic risk scores calculated using data from genome wide association studies  
92 (GWAS) suggests that an increased burden of common risk variants can act in concert with the  
93 22q11.2 deletion to further increase overall risk for psychosis<sup>23-25</sup>. These observations clearly

94 indicate the 22q11.2 deletion can at least act together with alterations in genetic pathways  
95 affected by additional risk variants. This raises the possibility that the deletion may converge on  
96 disease mechanisms that act in both ASD and schizophrenia.

97 We reasoned that finding the points of convergence between the effects of the 22q11.2  
98 deletion and other human genetic variants implicated in psychiatric disorders could provide a  
99 view into which genes present in the deletion, or pathways altered by it, contribute to mental  
100 illness. To identify such intersections, we opted to examine transcriptional changes in multiple  
101 stages of excitatory neuronal differentiation, given that genetic studies of ASD and schizophrenia  
102 have implicated genes that act during neuronal development and differentiation<sup>26-29</sup>, and in  
103 neuronal processes including excitatory transmission<sup>30-32</sup>. We therefore carried out RNA  
104 sequencing at three distinct stages of excitatory neuronal differentiation using induced  
105 pluripotent stem cells (iPSCs) from 22q11.2 carriers and non-carrier controls. In order to  
106 establish a causal link between the deletion and the transcriptional effects we also utilized gene  
107 editing to delete the chromosomal region in a control cell line. To robustly induce neuronal  
108 differentiation, we utilized an approach we previously described where Ngn2 expression<sup>33</sup> is  
109 coupled with forebrain patterning to produce homogenous populations of excitatory neurons with  
110 features similar to those found in the superficial layers of the early cortex<sup>34</sup>. We have previously  
111 characterized the cells generated by this approach using immunostaining, qPCR, single-cell RNA  
112 sequencing, whole-cell patch clamp, multi-electrode arrays and optical electrophysiology, and  
113 demonstrated reproducibility across multiple cell lines<sup>34-37</sup>.

114 Over the course of excitatory neuronal differentiation, we found that the 22q11.2 deletion  
115 acted in trans to significantly alter the expression of many genes with established genetic  
116 associations with neurodevelopmental disorders in progenitors, and schizophrenia in

117 differentiated neurons. To ask, in an unbiased manner, which pathways and genes were likely  
118 responsible for these changes, we developed an approach for identifying protein-protein  
119 interaction (PPI) networks that best explain a particular change in gene expression. This method,  
120 called PPItools, suggested that the 22q11.2 interval regulates the expression of genes in  
121 proliferative, presynaptic, proteasomal and JUN/FOS pathways. Finally, we found that cell lines  
122 with isogenic deletion of 22q11.2 recapitulated most of the changes observed in the patient-based  
123 cohort, including increased levels of the *MEF2C* transcription factor in neuronal progenitor cells  
124 and decreased expression of presynaptic proteins such as SV2A and NRXN1 in neurons.

125

## 126 **Results**

### 127 **Pilot study and power calculations**

128 The 22q11.2 deletion syndrome is associated with a wide spectrum of psychiatric  
129 conditions, which differ from person to person, and by age of diagnosis. To study the effects of  
130 the deletion, we both collected and derived hiPSC lines from patient carriers as well as non-  
131 carrier controls (Fig.1a-f, Extended Data Fig. 1a and Extended Data Table 1).

132 To estimate the sample size needed to be powered to detect gene expression changes, we  
133 performed a pilot study with two control and two 22q11.2 deletion iPSC lines, each from a  
134 distinct donor. The presence of the 3Mb 22q11.2 deletion provided an internal control with a  
135 built-in expectation for a set of known deleted genes and their anticipated magnitude of change.  
136 Thus, we reasoned this small study would allow us to detect the 50% reduction in the abundance  
137 of transcripts originating from within the deletion as well as changes in expression of genes  
138 outside of the deletion that were of a similar magnitude. We induced neuronal differentiation  
139 using a published, well-characterized approach, combining the overexpression of Ngn2 with

140 small molecule patterning<sup>37</sup> (Fig. 1g) , and completed RNA-sequencing at three cellular stages:  
141 human pluripotent stem cells (hPSCs, day 0 of differentiation), neuronal progenitor-like cells  
142 (NPCs, day 4 of differentiation)<sup>37</sup>, and in functional excitatory neurons displaying synaptic  
143 connectivity <sup>34</sup> (day 28 of differentiation) (Extended Data Table 1, Extended Data Fig. 1b-e).  
144 Following RNA-sequencing, we mapped reads to the Ensembl human genome assembly  
145 (GRCh37/hg19). We detected one or more reads for 51 protein coding genes that mapped to the  
146 22q11.2 deletion region, in the four lines at any one differentiation stage. On one hand, we were  
147 reassured to observe a systematic reduction in the abundances of RNAs encoded by genes  
148 mapping in the deletion, with the majority exhibiting fold-changes between -1.5 and -2 in  
149 deletion cells relative to controls. On the other hand, this decrease in RNA levels was  
150 indistinguishable from sample-to-sample variance on an individual gene level (after correcting  
151 for multiple testing), underscoring the limitations of a small sample size (Extended Data Fig. 1c-  
152 e). Only when we considered reads from the genes in the deleted region in aggregate could we  
153 observe a statistically significant reduction in gene expression between the deletion carriers and  
154 controls ( $p(\text{hPSCs}) = 4.13 \times 10^{-19}$ ,  $p(\text{NPCs}) = 1.58 \times 10^{-18}$ , and  $p(\text{neurons}) = 2.93 \times 10^{-15}$ , Mann-  
155 Whitney test).

156 Using our pilot sequencing data, we estimated that for genes expressed above the median,  
157 a sample size of > 20 carrier and > 20 control iPSC lines would yield on average >80% power to  
158 detect fold-changes of 1.35 across each of the three cell stages (Fig. 1h, Extended Data Fig. 1e,f).

159

## 160 **Profiling an expanded 22q11.2 cohort**

161 Guided by our power calculations, we assembled a collection of 20 (7 female, 13 male)  
162 22q11.2 deletion carrier and 29 (14 female, 15 male) control iPSC lines, each derived from a

163 distinct individual. It has been found that the size of the deletion doesn't seem to correlate with  
164 diagnosis or severity of the conditions, as patients with either the most common 3Mb deletion or  
165 smaller nested deletions appear to have similar diagnoses<sup>3,7,38,39</sup>. We thus decided to examine the  
166 impact of the deletion (agnostic to size or diagnosis) on gene expression during neuronal  
167 development. We performed RNA sequencing in hPSCs, NPCs and excitatory neurons for each  
168 of the 49 cell lines (in triplicates, N=441 total RNA sequencing libraries in mixed pools of both  
169 genotypes to minimize technical biases). With these data in hand, we revisited our initial power  
170 estimates and found that in the larger data set we achieved over 80% power to detect fold  
171 changes  $\geq 1.5$  of all detected protein coding genes (Extended Data Fig. 1h) across developmental  
172 stages.

173 Consistent with previous findings using the same neuronal differentiation approach<sup>34,37</sup>,  
174 differentiation down a neuronal trajectory resulted in a global change of gene expression  
175 between each cellular stage analyzed (day 0 iPSC, day 4 NPC, day 28 excitatory neuron).  
176 Principal component analysis (PCA) indicated that the primary component of variation between  
177 the samples was days of neuronal differentiation (PC1+2 = 46% of variance) (Fig. 1i, Extended  
178 Data Fig. 1g). We found close clustering of the samples from the 49 lines within a given  
179 differentiation time point within PC1 and PC2, suggesting a reproducible and reliable  
180 differentiation had occurred across the entirety of our experiments (Fig. 1g). This conclusion was  
181 supported by joint analysis of the data indicating that across the 49 cell lines, 4 pluripotency  
182 associated genes were robustly expressed at day 0 and then rapidly silenced, while 7  
183 representative NPC genes became expressed at day 4 with the strong emergence of 7 prototypical  
184 neuronal genes at day 28 (Fig. 2a, Extended Data Fig. 2c).

185

186 **22q11.2 effects on transcript abundance**

187 We next proceeded to ask the important question of how the 22q11.2 deletion status  
188 influenced gene expression during neuronal differentiation and first considered genes within the  
189 deletion. We observed a nominally significant reduction in RNA levels for 51 protein coding  
190 genes in the deletion region ( $p < 0.05$ , red and blue dots, Fig. 2c-e) with 49 of these transcripts  
191 yielding significantly reduced abundance in at least one time point (FDR  $< 0.05$ ) and 25  
192 significantly reduced in all 3 stages (FDR  $< 0.05$ ) (Fig. 2b, Extended Data Fig. 2a). These  
193 findings in excitatory neuronal cells were in line with previous reports using either mixed  
194 monolayer cultures of inhibitory and excitatory neurons carrying the 22q11.2 deletion<sup>40</sup> or  
195 organoids consisting of multiple cell types including glutamatergic neurons and astrocytes<sup>41</sup>. We  
196 found that for genes mapping to the deletion, which showed a significant change in their  
197 expression, the deletion genotype explained, on average, 42 to 52% of all variance in their  
198 expression (Extended data Fig. 3a-d). Included in these 49 significantly less abundant transcripts  
199 originating from the 22q11.2 locus, were seven that are highly intolerant for loss of function  
200 variants as measured by pLI score<sup>42</sup>, which ranks genes from most tolerant (pLI=0) to most  
201 intolerant (pLI=1). These seven genes that have a pLI score  $> 0.9$  (*UFIDL*, *HIRA*, *DGCR8*,  
202 *ZDHHC8*, *MED15*, *TBX1*) have been previously suggested to play role in some of the congenital  
203 phenotypes associated with the deletion in other tissues<sup>43</sup>. Together, our analyses indicate that  
204 our transcriptional phenotyping was sufficiently sensitive to allow the successful detection of the  
205 50% decrease in expression of the hemizygote genes found in the deletion region.

206

207

208

209 **Cell-type specific effects of 22q11.2 deletion**

210 After validating our ability to detect the altered expression of many genes within the  
211 deletion, we next explored differentially expressed transcripts originating from loci outside of the  
212 deletion. In fact, the majority (89%) of the genes differentially expressed in 22q11.2 carrier's  
213 cells were located outside the deletion region (n=383 genes) (Fig. 2b). In total, the trans effects  
214 of the deletion explained on average 18% of the total variance in gene expression across all data  
215 sets (Extended data Fig. 3a-d). Plotting the test statistic from the differential expression for every  
216 gene relative to its position in the genome suggested that there was no major positional clustering  
217 of differentially regulated genes to specific chromosomal regions outside the deletion area  
218 (Extended data Fig. 3e, day 28 example). Notably, only one gene, *CAB39L* on chromosome 13,  
219 was significantly induced in carriers at all stages (Extended Data Fig. 2b). Upon reviewing  
220 published data sets, we found that *CAB39L* expression was also induced in blood cells isolated  
221 from 22q11.2 deletion carriers<sup>44</sup>, suggesting that upregulation of this gene is likely to be  
222 associated with the 22q11.2 deletion in many cell types.

223 While genes within the 22q11.2 deletion region were regulated in the same direction at  
224 all developmental stages, the set of differentially expressed genes outside the deletion region was  
225 different for each stage. In contrast to the conserved downregulation of genes within 22q11.2  
226 across the three distinct time points we analyzed, except for *CAB39L*, the specific identity of the  
227 remaining differentially expressed genes was distinct at each differentiation stage assessed (372  
228 cell stage-specific genes). Importantly, the apparently discontinuous effects of the deletion  
229 between the cell stages were not the trivial result of certain transcripts failing to be detected  
230 because of barely falling outside a certain significance threshold. That is, in controls, the  
231 affected genes were expressed in all cell stages with little change in their overall average RNA

232 abundance between stages, ensuring reliable detection across all stages (Table S4 and Extended  
233 Data Fig. 4a,b). As a result, fold-changes in “trans” genes between carriers and controls were  
234 only modestly correlated between NPCs and hPSCs ( $\rho=0.28$ ,  $p=3 \times 10^{-8}$ ) and NPCs and neurons  
235 ( $\rho=0.23$ ,  $p=3 \times 10^{-6}$ ), while no correlation was observed between fold changes in hPSCs and  
236 neurons ( $\rho=0.06$ ,  $p=0.25$ ). Overall, these findings suggest that the 22q11.2 deletion has a  
237 temporally-dependent influence on gene expression, altering the abundance of distinct sets of  
238 transcripts as neuronal differentiation unfolds.

239 Lastly, our cohort included 18 cell lines with full length 22q11.2 deletion, along with two  
240 cell lines with nested 22q11.2 deletion. To verify that the cell lines with shorter deletion did not  
241 result in a different transcriptional signature, we repeated the differential gene expression  
242 analysis in day 28 neurons without the lines with short, nested deletions (SCBB-1430 and  
243 SCBB-1961, Table 1). We found that the differences in gene expression between the remaining  
244 deletion carriers and controls correlated strongly with those obtained in the complete data set  
245 ( $r=0.92$  for genes with adjusted  $p$ -value  $<0.05$ ), suggesting that the observed gene expression  
246 differences were robust also in the presence of the shorter deletions.

247

## 248 **Transcript alterations in hPSCs and NPCs**

249 The phenotypes that are found in a subset of 22q11.2 deletion carriers during early  
250 childhood<sup>3</sup> led us to ask if the genes we identified to be differentially expressed in deletion  
251 carriers at initial differentiation stages (hPSCs and NPCs) were genetically associated with  
252 neurodevelopmental disorders, including autism and intellectual disability. We included likely  
253 disease-causing genes from the Deciphering Developmental Delay (DDD) project, and a recent,  
254 large exome-sequencing study in autism (n=295 total neurodevelopmental disorders, NDD,

255 genes)<sup>27,45,46</sup> (Table S5). Of the 432 genes we found differentially expressed in deletion carriers,  
256 10 were NDD genes (hPSCs: *FOXG1*, *ELAVL3*; NPCs: *PAX6*, *MEF2C*, *FOXP2*, *NR2F1*, *MAF*,  
257 *PAX5*; neurons: *KMT2C*, *MKX*; OR = 1.85, p=0.046 (for all 432 genes) (Tables S1-S3). We took  
258 particular note of *MEF2C* as it is also implicated in schizophrenia through GWAS<sup>47</sup> and is  
259 known to encode a transcriptional regulator that participates in activity-dependent regulation of  
260 immediate early genes such as *JUN* and *FOS*<sup>48</sup>. *MEF2C* has been shown to be repressed by the  
261 transcription factor *TBX1*, which is encoded by a gene within the 22q11.2 interval<sup>49,50</sup>.

262 Proteins encoded by genes harboring causal mutations for a particular phenotype in  
263 Mendelian disorders have been shown to have more physical connections between one another  
264 than unrelated proteins<sup>51</sup>. We therefore wondered whether the transcripts expressed from within  
265 the 22q11.2 deletion and the transcripts with altered abundance in trans in deletion carriers  
266 encoded proteins that together had more than the expected number of interactions with proteins  
267 originating from loci genetically linked with NDD. As this is a question of broader relevance for  
268 connecting protein interaction data, changes in gene expression, and genetic data, we wrote a  
269 software package (PPItools, <https://github.com/alexloboda/PPItools>) to enable this analysis.

270 In this instance we used PPItools to identify the protein-protein interactions (PPI) from  
271 the InWeb database<sup>52</sup> of the differentially expressed gene products that we identified at each  
272 stage of neural differentiation and analyzed them for an apparent excess of genes implicated in  
273 NDD in this network. We used a curated list of NDD genes that comprised 295 genes that have  
274 been previously reported to have excess of deleterious variants in patients with ASD, and ID  
275<sup>45,46,53</sup> (Table S5). To ask whether this enrichment for NDD implicated interacting proteins was  
276 likely to have occurred by chance, we performed 1000 random permutations of sets of expressed  
277 proteins of the same size while constraining the scale and complexity of the network. These

278 analyses confirmed that genes we found to be differentially expressed early in differentiation (in  
279 hPSCs and NPCs) were significantly more likely to interact with gene products associated with  
280 NDD ( $p<0.001$ , Extended Data Fig. 4c). While there remained a modest enrichment for  
281 differentially expressed genes in excitatory neurons for interaction with NDD gene products, this  
282 enrichment was not significant.

283 To further control our observation, we asked whether the protein interaction network we  
284 identified at each time point showed any enrichment for genes linked with an unrelated  
285 condition, inflammatory bowel disease (IBD), or with a neurological condition, Parkinson's  
286 Disease (PD). As expected, there were no significant enrichments for IBD related gene products  
287 within the protein interaction networks identified at any of the differentiation time points  
288 analyzed, and no enrichment for PD related gene products in NPCs or neurons (Extended Data  
289 Fig. 4c, Table S5). Thus, our results demonstrate that within hPSCs and NPCs, there is indeed a  
290 convergence between genes within the 22q11.2 deletion and the transcripts altered in trans by the  
291 deletion with genes products that when mutated cause human neurodevelopmental disorders.

292

### 293 **Schizophrenia heritability enrichment in neurons**

294 Given that we had found an initial convergence between the effects of the 22q11.2  
295 deletion and the abundance of certain transcripts linked through rare variant analyses to NDD as  
296 well as with a broader collection of PPI networks implicated in NDD, we next proceeded to ask  
297 whether the transcripts that we had found to be altered in deletion carrier cells were enriched for  
298 additional genetic signals in mental illness. To investigate this possibility, we utilized the genes  
299 we identified to have significantly altered expression ( $FDR < 0.05$ ) in differentiating cells from  
300 22q11.2 carriers as a substrate for linkage disequilibrium (LD)-score regression<sup>30</sup>. For this

301 analysis we used GWAS summary statistics from the psychiatric genomics consortium (PGC), as  
302 well as educational attainment studies<sup>54-59</sup> to ask whether variants in 22q11.2-differentially  
303 expressed genes and their surrounding genomic regions contribute disproportionately to the  
304 polygenic heritability of five neuropsychiatric disorders (schizophrenia, bipolar disorder, major  
305 depressive disorder, autism spectrum disorder, and ADHD) . We applied two statistics to  
306 estimate heritability enrichment in LD-score regression: per-SNP heritability and total  
307 heritability enrichment. We found suggestive evidence for a modest increase in per-SNP  
308 heritability for schizophrenia among genes differentially expressed in neurons  $\tau_c=6.1 \times 10^{-8}$ ;  
309 p=0.0088 for 196 genes, FDR <5% and  $\tau_c=1.5 \times 10^{-8}$ ; p= 0.01 after examining all 4,192 genes  
310 with nominally significant differences in expression, p<0.05, 2,864 up genes and 1,328 down  
311 genes, respectively) (Fig.3a). Analysis of up- and down-regulated genes (p<0.05) separately  
312 revealed that the increase in the per-SNP heritability was accounted for by transcripts that were  
313 more abundant in deletion carrier neurons (p ( $\tau_c$ )=  $4.2 \times 10^{-6}$  p(Bonferroni)=0.0003) (Fig.3a,  
314 Table S6). Our findings were unlikely to be the result of neurons merely expressing increased  
315 levels of genes relevant for these psychiatric conditions: permutation with 100 random gene lists  
316 produced from our neuronal data and matched for expression level, indicated that the per-SNP  
317 heritability enrichment in genes we found to be induced in deletion carrier neurons was ~10,000-  
318 times more significant than any random gene set (Extended Data Fig.5a-c). We found a similar  
319 trend when examining the total heritability accounted for by variants in these genes, where we  
320 found an increase in heritability enrichment for bipolar disorder and educational attainment in  
321 addition to schizophrenia (Extended Data Fig. 5d,e, Table S6).

322 To again query the relationship between differentially expressed genes in 22q11.2  
323 deletion neurons and common genetic variants more broadly associated with psychiatric illness,

324 but with a different set of statistical assumptions, we applied multiple-regression for competitive  
325 gene-set analysis in MAGMA-software<sup>60</sup>. Like results from the LD-score regression analysis,  
326 genes whose transcripts were more abundant in 22q11.2 deletion neurons were more strongly  
327 associated with schizophrenia than the rest of the genome ( $p=5.6 \times 10^{-7}$ ,  $p(\text{Bonferroni})=4.03 \times$   
328  $10^{-5}$ ) (Extended Data Fig. 6a). Altogether, 20 genes with nominally significant gene-wise  
329 association to schizophrenia from MAGMA ( $p_g < 0.05$ ) were significantly differentially expressed  
330 in deletion neurons (Fig. 3b, Extended Data Fig. 6c). Repeating the analysis with 100 random  
331 gene lists generated from our expression data confirmed that this result was unlikely to have  
332 arisen merely as a result of examining these neuronal cells (Extended Data Fig. 6b).

333 To determine if this association between 22q11.2 deletion induced genes and  
334 schizophrenia heritability was replicable and to determine the specificity of this signal, we used  
335 summary statistics from an independent GWAS dataset of 650 heritable traits from the UK-  
336 biobank. Strikingly, LD-score regression showed the genes upregulated in 22q11.2 deletion  
337 neurons harbored significant heritability enrichment for schizophrenia, but not for the other traits  
338 (Fig.3c). Overall, our findings indicated that excitatory neurons harboring the 22q11.2 deletion  
339 exhibited increased abundance of transcripts from genes that underlie schizophrenia heritability,  
340 but that the deletion did not have such a detectable effect at earlier stages of differentiation.

341

### 342 **Schizophrenia rare variant enrichment in neurons**

343 Exome sequencing at increasing scale has begun to reveal a burden of rare protein  
344 damaging variants in schizophrenia patients, complementing the genetic signal of common  
345 regulatory variants emerging from GWAS<sup>61-63</sup>. In contrast to the common variant polygenic risk,  
346 which arises incrementally from many small-effect variants, the schizophrenia-associated rare

347 variants identified so far act with strong individual effects. While there is evidence for common  
348 and rare risk variants in schizophrenia mapping to shared chromosomal intervals<sup>32</sup>, so far the two  
349 forms of variation implicate largely distinct sets of genes. We therefore asked whether the  
350 22q11.2 deletion also effects the expression of genes that harbor rare coding variants, identified  
351 by the schizophrenia exome meta-analysis consortium (SCHEMA) in schizophrenia patients<sup>63-65</sup>.  
352 We initially focused on genes upregulated in neurons from 22q11.2 carriers (n=2,864 genes at p  
353 < 0.05) and used 100 random gene lists matched for their expression levels in our excitatory  
354 neurons as controls. This analysis revealed two interesting results: First, alterations in the  
355 expression of genes harboring a burden of loss of function mutations in schizophrenia were  
356 significantly enriched in excitatory neurons from 22q11.2 carriers (Fig. 3d red dots, 57/100  
357 random gene lists assessed p <0.05). Second, that the 2,864 transcripts within these neurons  
358 whose expression were increased in 22q11.2 deletion carriers were substantially more  
359 significantly enriched for loss of function variants than any of the random gene lists we sampled  
360 (Fig. 3d, red dot black circle; p = 1.29x10<sup>-12</sup>). This enrichment signal was substantially reduced  
361 for missense mutations in schizophrenia patients and absent for synonymous variants (green and  
362 blue dots Fig. 3d). We further examined the differential expression results for genes with  
363 significant burden of deleterious mutations in schizophrenia patients in SCHEMA. One transcript  
364 encoded by *ZMYM2* out of 32 significant genes from SCHEMA was significantly changed in the  
365 deletion lines (FDR<5%). Seven additional genes (*RB1CC1*, *AKAP11*, *ASHIL*, *GRIA3*, *SV2A*,  
366 *PCL0*, *DNM3*) were nominally significantly changed in the deletion neurons. Remarkably, all  
367 eight SCHEMA genes were upregulated in the deletion carrier neurons.

368 Consistent with the notion that we were analyzing a disease relevant cell type, our rare-  
369 variant burden analyses indicated that the excitatory neurons we produced from both cases and

370 controls expressed a significant excess of genes harboring rare pathogenic coding variants in  
371 schizophrenia patients. However, our analysis further indicated that in excitatory neurons the  
372 22q11.2 deletion was specifically associated with alterations in a set of genes that were even  
373 more markedly enriched for rare loss of function variants in schizophrenia patients (Fig. 3d,  
374 circled dot). Like our common variants analyses, genes whose expression we found altered in  
375 pluripotent stem cells and NPCs harboring the 22q11.2 deletion did not exhibit this excess of rare  
376 coding variants schizophrenia (Extended data Fig. 7a, Table S7).

377

### 378 **Protein-protein interaction networks associated with transcriptional changes**

379 As the number of trans acting effects of the deletion on transcripts linked to psychiatric  
380 illness were substantial, we sought an unbiased approach for identifying the pathways that could  
381 be contributing to their alterations. Ideally, such a method would also have the capacity to  
382 identify potential connections to gene products originating from within the deletion interval  
383 itself. To this end, we used PPI data<sup>52</sup> to search for the smallest number of biochemical  
384 interactions that could explain the most prominent transcriptional changes in deletion carriers. To  
385 facilitate this effort, we developed a new tool (included in the R-package “PPItools”, see  
386 methods) that scores observed p-values from differential expression to construct a node weighted  
387 graph with the strongest cumulative association with the deletion genotype at each cell stage  
388 (most-weighted connected subgraph, MWCS). We then performed 1000 permutations on p-  
389 values from differential expression while preserving the node degrees, to ensure that the  
390 connected gene-products were unlikely to occur in the subgraph by chance alone ( $p < 0.05$ , Table  
391 S8) (Extended Data Fig. 8a). This analysis revealed that the minimal interaction networks for  
392 each of the three stages of differentiation were predominantly composed of proteins encoded by

393 genes located within the 22q11.2 deletion, that were in turn interconnected with proteins encoded  
394 by genes residing outside of the deletion (Extended Data Fig. 8b,c and Fig. 4g).

395 In pluripotent stem cells, we found that the most weighted subgraph contained 53 node  
396 proteins, 26 of which were encoded by genes mapping to the deletion (Extended Data Fig. 8b).  
397 These nodes were organized around several hub proteins encoded by genes that map outside the  
398 deletion. These included MYC, p53 (TP53) and the autism associated protein p21 (CDKN1A)  
399 suggesting that the deletion disrupts regulation of the cell cycle and directly impacts expression.  
400 Our analyses suggest alterations in the expression of these well-known cell cycle regulators  
401 could be mediated by reduced expression of several interacting proteins that map to the deletion  
402 including CDC45, a regulator of DNA replication, TRMT2A, which encodes a known cell cycle  
403 inhibitor, as well as LZTR1 a known tumor suppressor. Another notable hub observed in stem  
404 cells was that encoding the low affinity nerve growth factor receptor and known NOGO Co-  
405 receptor P75, which was increased in expression. The minimal network implicated the NOGO  
406 receptor (RTN4R) and the mediator of protein degradation through the proteasome UFD1L, both  
407 of which are encoded within the deletion.

408 In neural progenitor cells (Extended Data Fig. 8c), we continued to see evidence for  
409 disruption in NOGO signaling through increased expression of both NOGO (RTN4) and the  
410 TRKA receptor, which is associated with autism through rare protein-coding variation and is also  
411 a known interactor with P75 and whose signaling is modulated by NOGO signaling. These  
412 findings suggest that reduced expression deletion proteins such as the NOGO receptor and less  
413 appreciated interacting proteins encoded within the deletion such as PIK4A and ARCV4 are  
414 disrupting signaling. Another significant signal emerging from the minimal network in NPCs  
415 was for a disruption in RNA metabolism. This was exemplified by a hub centered around The

416 TFIID transcription factor, TAF1 which interacted with the tumor suppressor proteins LZTR1  
417 and LZTS2, the transcriptional activator NFKBIA, an RNA helicase associated with ASD,  
418 MOV10, and GNB1L, encoded within the deletion, with roles in cell cycle progression and gene  
419 regulation. TAF1 was also connected to the protein-ubiquitination pathways via interactions with  
420 HSPA1B and its interactors, both from within and outside the deletion region.

421 In neurons (Fig. 4g), we identified three major hubs consisting of 1) interactors of the  
422 activity-dependent transcription factor *JUN*, including the proteasome subunit PSMD12 and the  
423 kinesin KIF2A, both associated with NDD, and BANP, a cell cycle regulator, along with several  
424 proteins encoded in the 22q11.2 interval: TRMT2A, RANBP1, GNB1L, MRPL40, SCL25A1,  
425 CRKL, with connections to the transcriptional (POLR2A) and chromatin remodeling (HIRA)  
426 machineries; 2) components of the protein ubiquitination / metabolism pathway, including  
427 SMAD2, COPS5 and WWP2 along with UFD1L, KLHL22, both encoded within the deletion  
428 region; and 3) synaptic vesicle trafficking, including CLTCL1 encoding clathrin, the  
429 synaptobrevin VAMP2, which is associated with NDD, and SNAP29 located in the 22q11.2  
430 locus and encoding a synaptosome associated protein (Fig. 4g). Overall, our analyses support the  
431 notion that multiple distinct but connected pathways are at the core of the transcriptional changes  
432 that we observe in deletion carrier neurons: activity-dependent gene expression, protein  
433 homeostasis, and synaptic biology.

434

#### 435 **Enrichment of synaptic and protein homeostasis ontologies in deletion altered transcripts**

436 We next wondered how changes in gene expression caused by the 22q11.2 deletion might  
437 impact neurobiological processes. To this end, we employed recently reported synaptic gene  
438 ontologies<sup>31</sup> to search for potentially converging synaptic biology among the genes differentially

439 expressed in 22q11.2 patient neurons. Strikingly, 239 of the 2,864 transcripts with increased  
440 abundance in 22q11.2 neurons possessed a synaptic process annotation in SynGO<sup>31</sup>  
441 ( $p=1.1 \times 10^{-10}$ ), with a particular enrichment for transcripts with presynaptic functions in  
442 synaptic vesicle cycle (GO:0099504,  $p_{FDR \ adj}=6.12 \times 10^{-9}$ , Fig. 4a, Table S9), while 35 of the  
443 1,328 downregulated transcripts, including five cis genes, had a SynGO annotation. We next  
444 wondered whether these 239 synaptic genes were a major contributor to the schizophrenia  
445 heritability enrichment we detected in the overall set of transcripts induced in deletion neurons.  
446 Indeed, we found a marked reduction in the per SNP heritability for schizophrenia after  
447 removing these 239 transcripts from the 2,864 that showed increased abundance in 22q11.2  
448 deletion neurons (Fig. 4b). This reduction was greater than that observed when randomly drawn  
449 lists of 239 transcripts were removed from the overall pool of 2,864 more abundant transcripts,  
450 suggesting that this modest number of synaptic transcripts explained proportionally more of the  
451 heritability than the rest.

452 A further gene ontology enrichment analysis revealed that genes induced in 22q11.2  
453 neurons were significantly enriched for functions particularly in the protein ubiquitination  
454 pathway (GO:0000209, 87 genes, OR=2.13,  $q = 7.5 \times 10^{-8}$ ) and with the largest individual  
455 enrichment for regulation of synaptic vesicle exocytosis (GO:2000300, 14 genes OR=4.0,  $q$   
456  $=2.3 \times 10^{-4}$ ) (Table S10). This enrichment with functions in protein homeostasis and synaptic  
457 signaling was specific for induced genes in neurons. Conversely, in the genes induced in earlier  
458 developmental stages, the enriched functions were related to developmental processes, including  
459 tube morphogenesis and development, along with cell motility, migration and differentiation in  
460 hPSCs and embryonic development and cardiac epithelial to mesenchymal transition in NPCs.  
461 In comparison, genes reduced by the deletion in neurons highlighted exclusively functions in

462 cilium assembly (GO:0060271, 54 genes, FC= 2.2,  $q = 6.4 \times 10^{-5}$ ), while genes reduced in  
463 hPSCs and NPCs were not enriched for any biological processes (Tables S11-S13). Together the  
464 results of our gene ontology and PPI analyses converge on the same key pathways that are  
465 regulated by the 22q11.2 deletion in each cell type. These results further demonstrate that the cell  
466 type-specific effects of the deletion involve distinct biological functions that may have clinical  
467 relevance for the phenotypic presentation in patients.

468

#### 469 **Enrichment for programs associated with activity dependent gene expression**

470 To further investigate which cellular programs might mediate the changes in synaptic  
471 gene expression and protein homeostasis observed upon 22q11.2 deletion, we carried out motif  
472 enrichment analysis on the genes upregulated ( $p < 0.05$ ) in deletion carrier neurons to identify  
473 transcription factor binding motifs that are enriched in this gene set. The motif that was most  
474 significantly enriched was for binding of the *JUN/FOS* transcription factors (1.6-fold  
475 enrichment,  $p = 10^{-14}$ ; Fig. 4c, Table S14). The *JUN* and *FOS* transcription factors are immediate  
476 early genes that are activated in response to neurotransmitter release and activate a downstream  
477 “activity-dependent” transcriptional cascade to regulate downstream programs, such as protein  
478 homeostasis and synaptic transmission<sup>48</sup>.

479 Notably, there was significant overlap ( $p = 5.57 \times 10^{-16}$ ) between the genes altered in  
480 deletion neurons that had synaptic ontologies (Table S9) and the altered genes that were targets  
481 of *JUN/FOS* (Table S14) suggesting that activity dependent gene expression downstream of  
482 *JUN/FOS* is a contributor to the synaptic signal that we detected in 22q11.2 deletion neurons.  
483 Additionally, a further gene ontology enrichment analysis of the unique *JUN/FOS* targets we

484 identified (Table S14) revealed an enrichment of components of the protein ubiquitination  
485 pathway (GO:0016567, 29 genes, OR=2.9,  $p_{FDR\ adj}= 0.00098$ , Table S15).

486 Furthermore, transcript levels of *MEF2C*, an activity-dependent transcription factor  
487 acting upstream of the *JUN* / *FOS* signaling pathway to regulate the expression of immediate  
488 early genes<sup>48</sup>, are increased in 22q11.2 deletion carrier NPCs in our discovery dataset (Table S2,  
489 Fig. 4d, and validated by qPCR and immunoblotting, Extended Data Fig. 2f,g). *MEF2C* has been  
490 shown to negatively regulate synaptic transmission by restricting the number of excitatory  
491 synapses<sup>66,67</sup>. Additionally, *TBX1*, a transcription factor located in the 22q11.2 deletion region  
492 and significantly downregulated in these same NPCs (Extended Data Fig. 2d,e), is a known  
493 repressor of *MEF2C*<sup>49,50</sup>. Thus, decreased *TBX1* levels due to loss of a copy of 22q11.2 likely  
494 result in de-repression of the *MEF2C* transcription factor, a regulator of the *JUN/FOS* signaling  
495 pathway, which in turn might reduce synaptic transmission.

496 Taken together, these results indicate that activity dependent gene expression is changed  
497 in deletion carrier cells, likely impacting downstream protein homeostasis and synaptic  
498 transmission.

499

## 500 **Reduced network activity in 22q11.2 deletion neurons**

501 Overall, our data suggests that changes linked to the 22q11.2 deletion during the  
502 development of excitatory neurons alter the balance of the *JUN/FOS* transcriptional pathway,  
503 which has well established roles in activity dependent gene expression<sup>48</sup>. We thus hypothesized  
504 that the transcriptional activation of this pathway and its targets, which plays a role in reducing  
505 synaptic transmission upon sustained activity<sup>48</sup> might result in decreased network activity in  
506 neuronal cultures with 22q11.2 deletion.

507 We thus asked whether neurons from 22q11.2 deletion carriers exhibited changes in  
508 network activity. Previously, we had shown that by 42 days of excitatory differentiation, neurons  
509 derived from control cell lines were spontaneously active and that their rate of firing was  
510 governed almost entirely by network activity mediated through synaptic connectivity<sup>34</sup>. We used  
511 multielectrode arrays (MEAs) to monitor neuronal network development and activity over 42  
512 days of neuronal differentiation<sup>34</sup>. In neurons derived from patients with 22q11.2 deletion, we  
513 detected a significantly lower spiking rate from 21 days of differentiation and onward, when  
514 compared to controls (N = a total of 162 wells from 21 cell lines) (Fig. 4e,f). We found this  
515 result striking, as it was consistent with the notion that the altered abundance of synaptic  
516 transcripts and activity-dependent gene expression we observed by RNA sequencing was  
517 associated with functional effects on network activity in 22q11.2 deletion neurons.

518

### 519 **Gene editing of the 22q11.2 deletion**

520 To complement our patient driven study and assess whether the 22q11.2 deletion was  
521 sufficient to explain the transcriptional changes we observed in our patient-based discovery  
522 cohort, we used CRISPR/Cas9 to engineer the 22q11.2 deletion in a human embryonic stem cell  
523 line (H1/WA01). Using guide RNAs that cut within the low copy repeats (LCRs) flanking the  
524 3Mb 22q11.2 deletion, we generated heterozygous 22q11.2 deletion cell lines at a very modest  
525 frequency (2/1000), as well as many non-targeted but otherwise isogenic controls (Fig. 5a-d). We  
526 then subjected the two deletion clones and two non-targeted control clones to neuronal  
527 differentiation and performed RNA sequencing at the same differentiation stages we assessed  
528 previously (d0 hPSCs, d4 NPCs and d28 excitatory neurons). In PCA, components one and two  
529 separated each of the samples by differentiation state, with the stem cell, NPC and neuronal cell

530 lines showing strong reproducibility of differentiation across replicates (Fig. 5e). Impressively,  
531 components three and four then separated each of the samples based on their deletion status, with  
532 22q11.2 deletion samples substantially separated from their non-targeted counterparts (Fig. 5f,  
533 Extended Data Fig. 9a). This separation was not solely due to deleted cis genes as it persisted  
534 upon removal of these genes from the PCA, indicating that it was a more global phenomenon in  
535 the transcriptome of the edited lines. Importantly, the genes driving the separation in PC3 and  
536 PC4 were largely shared by those detected differentially expressed in the discovery cohort. Out  
537 of the top 100 negative and positive loadings for PC3, 79 and 83, respectively, were nominally  
538 significantly changed also in neurons in the discovery cohort ( $p < 0.05$ ). For PC4, this overlap  
539 was 39 and 60 out of 100, for negative and positive loadings, respectively.

540 We next proceeded to perform differential expression analysis to delineate transcriptional  
541 changes present in clones edited to contain the 22q11.2 deletion (Tables S16-S18). As expected,  
542 the edited lines showed systematic downregulation of genes in the deletion region at all cell  
543 stages ( $p = 6 \times 10^{-61}$ , Mann-Whitney test) (Fig. 5g) with 26, 25, and 29 deleted genes passing  
544 individually FDR < 5% cutoff in the isogenic hPSCs, NPCs, and neurons. This further confirmed  
545 successful introduction of the heterozygous 3Mb deletion in this background. Notably among  
546 these and like the discovery set, *CAB39L* was consistently upregulated at all differentiation  
547 stages in lines with isogenic 22q11.2 deletion. Overall, we also observed a highly significant  
548 number of genes exhibited aligned changes in transcript abundance between the discovery cohort  
549 and edited samples ( $p < 0.05$ ) across all differentiated stages analyzed: hPSCs, 75% (200 out of  
550 268  $p = 3 \times 10^{-16}$ , binomial test); NPCs, 83% (124 out of 150  $p = 1.7 \times 10^{-16}$ , binomial test) and  
551 neurons, 76% (604 out of 791  $p = 5.6 \times 10^{-9}$ , binomial test) with strongly correlated effect sizes  
552 ( $r_{hPSC} = 0.7$ ,  $r_{NPC} = 0.82$ ,  $r_{neuron} = 0.56$ , Pearson correlation); (Fig. 5h, Extended Data Fig. 9b,c).

553 We next wondered whether the pathways and cellular programs that were altered in a  
554 cell-type specific manner in our discovery dataset were also altered in the edited lines. To this  
555 end, we examined the expression of genes contributing to the minimal PPI networks identified at  
556 each cell stage in the discovery dataset (Fig 4g and Extended Data Fig. 8) and found that an  
557 overwhelming majority of these genes are changed in the same direction in cells with isogenic  
558 22q11.2 deletion at each stage, with 90%, 88% and 86% of the genes contributing to the PPI  
559 network in stem cells, NPCs and neurons respectively, being altered in the same direction in the  
560 isogenic dataset compared to the discovery dataset. Notably, the activity dependent gene  
561 *MEF2C* was also increased in NPCs of H1 deletion carrier cells compared to isogenic controls  
562 (Fig. 5i, Extended Data Fig. 9d,e).

563 Furthermore, upon synaptic process annotation in SynGO we observed a replication of  
564 the induction of genes ( $p < 0.05$ ) involved in synaptic vesicle cycle and endocytosis in the edited  
565 neurons with 22q11.2 deletion (GO: 0099504,  $p_{FDR\ adj} = 0.0029$ ) (Fig. 5j, Table S19). Overall, of  
566 the 239 transcripts with synaptic functions in the discovery dataset (Fig. 4a), 49 were also more  
567 abundant in neurons ( $p < 0.05$ ) harboring the engineered 22q11.2 deletion (Expected = 39 genes,  
568  $p < 0.012$ , binomial test), out of which 21 passed the FDR  $< 5\%$  cutoff for significance.

569 Additionally, the 87 transcripts implicated in the ubiquitination pathway that we found to  
570 be more abundant in 22q11.2 deletion carrier neurons were on average 0.29 standard deviations  
571 (SDs) higher expressed in the edited lines (95%-CI: 0.18-0.41 SDs,  $p = 3.9 \times 10^{-7}$ , t-test).  
572 Moreover, 19 of these transcripts were individually significantly (FDR  $< 5\%$ ) more abundant  
573 after gene editing of the deletion ( $p = 0.03$  binomial test) supporting a causative connection  
574 between the deletion genotype and altered transcript abundance for components in the ubiquitin-  
575 proteasome system in neurons. Furthermore, 28 out of the 99 JUN target genes induced in the

576 discovery dataset were also induced in neurons with isogenic 22q11.2 deletion ( $p < 0.05$ ) ( $p =$   
577 0.00046, binomial, expected overlap = 14 genes). Finally, encouraged by the replication of the  
578 differential expression signal in the edited deletion lines, we examined these genes ( $p < 0.05$ ) for  
579 association to schizophrenia. Remarkably, variants surrounding the induced genes in the edited  
580 lines revealed significant gene-wise association to schizophrenia consistent with the observation  
581 in the discovery cohort ( $\beta = 0.11$ ,  $SE = 0.029$ ,  $p = 6.6 \times 10^{-5}$ ,  $N = 1611$  genes, MAGMA). Thus, we  
582 conclude that the 22q11.2 deletion is indeed sufficient to explain most transcriptional effects we  
583 found to be associated with the deletion in our case-control cohort, including those related to the  
584 genetic risk for schizophrenia.

585

#### 586 **Reduced pre-synaptic protein abundance in 22q11.2 deletion neurons**

587 As an independent means of examining whether the 22q11.2 deletion impinged on  
588 presynaptic components in excitatory neurons, we performed whole cell proteomics on day 28  
589 neurons from two patients and two controls (Fig. 6a) As expected, peptides mapping to genes  
590 within the 22q11.2 interval were reduced in neurons harboring the deletion relative to levels in  
591 controls (Fig. 6b; Table S20).

592 Importantly, consistent with the altered expression of activity-dependent genes (Fig.  
593 4c,d,g and Table 14), and the reduced synaptically-driven network activity in 22q11.2 deletion  
594 neurons (Fig. 4 e,f), we found that proteins downregulated in 22q11.2 deletion neurons were  
595 enriched for synaptic gene ontologies (Fig. 6c). In total, 184 of the proteins that were  
596 downregulated in deletion carrier neurons had SynGO annotations. Of these, 68 were  
597 upregulated at the transcriptional level. Additionally, 31 proteins were upregulated in deletion

598 carrier neurons and had SynGO annotations; 4 of which were also upregulated at the mRNA  
599 level (Extended Data Fig. 9f).

600 The synaptic components exhibiting alterations in deletion neurons were predominantly  
601 presynaptic and specifically involved in synaptic vesicle cycle ( $p_{FDR\ adj} = 3.5 \times 10^{-19}$ ) (Fig. 6c;  
602 Table S21), and included Synaptotagmin 11 (SYT11), Neurexin-1 (NRXN-1), and Synaptic  
603 Vesicle Glycoprotein 2A (SV2A). SV2A (Fig. 6d) regulates vesicle exocytosis into synapses  
604 and works in presynaptic nerve terminals together with Synaptophysin and Synaptobrevin<sup>68,69</sup>.  
605 We note this finding also converges with genetic studies as rare variants in SV2A have been  
606 shown to be significantly associated with schizophrenia<sup>65,70</sup>. Similarly, *NRNX1* has established  
607 roles in schizophrenia<sup>65,71,72</sup> and *SYT11*, located on the chromosome locus 1q21-q22 may be a  
608 risk gene for schizophrenia<sup>73</sup>. We confirmed the decreased expression of SV2A (Fig. 6e), along  
609 with the reduction of protein levels of SYT11 (Extended Data Fig. 9g) and NRXN1 (Extended  
610 Data Fig. 9h) in 22q11.2 deletion neurons by immunostaining or immunoblotting. Additional  
611 proteins with schizophrenia rare variant associations (via the SCHEMA consortium<sup>65</sup>) altered in  
612 22q11.2 deletion neurons included DNM3, MAGI2 and TRIO (downregulated in patient  
613 neurons) and HIST1H1E, SRRM2 and ZMYM2 (upregulated in patient neurons) (Table S21).

614

## 615 **Discussion**

616 Here we have explored the transcriptional and functional consequences of the 22q11.2  
617 deletion on human neuronal differentiation. Our findings lead to several new insights into the  
618 biology of 22q11.2 deletion syndrome and how it confers risk for the development of varied  
619 psychiatric disorders as neural development and differentiation unfold. Notably, we found that  
620 the genes whose expression is perturbed in deletion carriers directly connect the effects of the

621 deletion on neuropsychiatric phenotypes to genes and pathways implicated in NDD, ASD and  
622 schizophrenia through prior large-scale exome sequencing and GWAS studies<sup>27,28,32,45-47,63,64,74</sup>.  
623 Thus, rather than working through independent mechanisms, our studies suggest the deletion  
624 confers risk for these various conditions at least in part by converging on the same gene products  
625 and pathways that are more widely disturbed in other patients.

626 We used a new tool that we developed and report here to ask which minimal PPI  
627 networks best explain the changes in gene expression we observed. This analysis revealed that a  
628 surprising number of deletion components likely play a role in the transcriptional signals. We  
629 therefore propose a model in which reduced abundance of multiple factors within the deletion  
630 region leads to highly distributed effects on many genes outside the deletion. Through the course  
631 of development, the deletion affects distinct sets of genes. In stem cells and neuronal progenitor  
632 cells the deletion impacts pathways linked to proliferation, NOGO signaling and RNA  
633 metabolism. In neurons, the deletion alters activity-dependent gene expression, protein  
634 homeostasis and ultimately, presynaptic biology. Overall, it was notable that *MEF2C*, an  
635 activity dependent transcription factor and negative regulator of excitatory synaptic density<sup>66,67</sup> is  
636 overexpressed in NPCs with 22q11.2 deletion, likely due to the loss of one copy of *TBX1*, a  
637 known *MEF2C* inhibitor located in the 22q11.2 interval<sup>49,50</sup>. Increased expression of *MEF2C*,  
638 could, in turn, lead to premature activation of the JUN and FOS pathway, which would be  
639 predicted to result in reduced network activity and synaptic connectivity.

640 To directly test this idea, we examined whether neurons from 22q11.2 deletion carriers  
641 displayed reduced synaptic functionality. Using a network activity assay in these cells, which we  
642 have previously shown was largely driven by a mixture of AMPA and NMDA receptor mediated  
643 transmission<sup>34</sup>, we indeed found this to be the case. Many of the patients' neurons showed a

644 significant overall reduction in network activity relative to controls. Thus, the deletion was not  
645 only associated with induction of activity dependent gene expression, but also associated with  
646 aligned changes in neuronal function. Based on these findings, we would thus expect a decreased  
647 expression of synaptic proteins, which we do, indeed, detect.

648 Our proteomic examination of 22q11.2 deletion neurons afforded an orthogonal  
649 examination of synaptic components in these cells and independently identified significant  
650 presynaptic alterations, including alterations in components that we could not ascertain by RNA  
651 sequencing such as the schizophrenia associated gene SV2A, a key mediator of pre-synaptic  
652 function. This last result is of translational and therapeutic importance given the existence of a  
653 positron emission tomography (PET) radiotracer specific for SV2A based on the drug  
654 Levetiracetam which now enables the *in vivo* investigation of presynaptic protein levels in the  
655 patient brain<sup>75</sup>. Interestingly, a recent PET-imaging study utilizing this SV2A radiotracer found a  
656 significant reduction in the abundance of this presynaptic component in the cortex of  
657 schizophrenia patients relative to controls<sup>76</sup>. Careful genotyping of this schizophrenia patient  
658 population was not carried out prior to imaging and our results suggest that a more specific study  
659 examining SV2A levels in 22q11.2 deletion carriers of varying diagnoses would be warranted.

660 Early during neuronal differentiation, we found that a significant number of the genes  
661 differentially expressed in deletion carriers had been previously linked to damaging or LoF  
662 sequence variants more widely identified in NDD and ASD. This enrichment for overlap  
663 between broader genetic signals in ASD and the effects of the 22q11.2 deletion was very  
664 significant when we considered the known biochemical interaction partners of gene products  
665 implicated in ASD. These findings are consistent with smaller scale studies investigating

666 transcriptional effects of individual genes, such as *FOXP1* or *CHD8*, linked with autism, and  
667 found to regulate the expression of ASD-relevant pathways<sup>77,78</sup>.

668 Interestingly, as differentiation proceeded and cells took on a post-mitotic, excitatory  
669 neuronal identity, the effects of the 22q11.2 CNV on expression of genes outside of the deletion  
670 lost enrichment for genes implicated in NDD/ASD and acquired an enrichment for genes  
671 harboring rare inactivating exome variants preferentially associated with schizophrenia. The  
672 influence of the 22q11.2 deletion on expression of neuronal genes associated with schizophrenia  
673 was not limited to those impacted by rare schizophrenia mutations acting with large effect. We  
674 also found that the deletion affected neuronal genes that were in linkage disequilibrium with  
675 common genetic variants associated with schizophrenia, a result replicated using genotypic data  
676 from two independent GWAS studies. Just as signal from ASD/NDD associated genes was  
677 absent in the neuronal stage of differentiation, the enrichment for effects on schizophrenia  
678 associated genes was absent in stem cells and NPCs. This surprisingly selective signal is likely to  
679 reflect stage-specific cellular programs, such as synaptic processes (for example those listed in  
680 Tables S9, S19 and S20) being specific to neurons.

681 We found these transcriptional results striking as NDD and ASD are linked to biological  
682 processes acting early in brain development<sup>79</sup>, while sequence variants associated with  
683 schizophrenia have been previously shown to be enriched for genes expressed in excitatory  
684 neurons and more recently for genes functioning in excitatory synaptic transmission<sup>80</sup>. It is  
685 important to note that our findings were not merely the result of looking at a chance list of genes  
686 in cell types clearly impacted in these diseases. While we did find that the overall gene  
687 expression profile of our excitatory neurons was enriched for expression of genes implicated in  
688 schizophrenia, the specific transcripts induced by the 22q11.2 deletion showed significantly

689 greater enrichment in all tests we performed. Thus, we hypothesize that by looking in a human  
690 cell type with disease relevant biology, we were able to identify previously unappreciated effects  
691 of the 22q11.2 deletion.

692 Overall, our findings support human genetic studies suggesting that neuropsychiatric  
693 CNVs such as 22q11.2 deletion likely interact with risk variants in the genetic background<sup>23-25</sup>.  
694 Transgenic mice carrying syntenic deletions that model the human 22q11.2 deletion have  
695 produced a wealth of datasets around neurodevelopmental abnormalities linked to the deletion or  
696 to individual genes within the region<sup>13,20,81</sup>. It is, however, important to keep in mind that such  
697 transgenic mice do not have genetic backgrounds harboring human polygenic risk alleles, which  
698 explain the majority of heritable variation in schizophrenia and other psychiatric phenotypes<sup>47</sup>.  
699 Therefore, while non-human model systems offer invaluable biological insight, they fall short of  
700 reproducing human specific gene regulatory effects underlying complex human disorders.

701 Individual genes within the 22q11.2 region have been at the center of several studies  
702 aiming to identify causal genes underlying the 22q11.2 deletion syndrome. Several of these  
703 studies, using rodent, and more recently, human<sup>41</sup> models, have reported defects in synaptic  
704 processes and brain connectivity<sup>82-84</sup>, many with a focus on *Dgcr8*, which encodes a subunit of  
705 the microprocessor complex which mediates microRNA biogenesis<sup>13</sup>. Khan et al<sup>41</sup> identified a  
706 calcium signaling defect in organoids containing mixed cell types derived from 22q11.2 deletion  
707 and controls individuals, which could then be rescued by *DGCR8* overexpression. Whether these  
708 phenotypes can be recapitulated with a scaled sample set and defined cell types remains to be  
709 seen. At face value, alterations in *DGCR8* might seem like a promising candidate for the  
710 distributed effects on gene expression we observed across many transcripts. However, reduced  
711 microRNA function from lower *DGCR8* copy number would predict an increased rather than

712 decreased abundance of the synaptic proteins we found. Another candidate, *DGCR5*, which  
713 encodes a long non-coding RNA within the 22q11.2 interval, has previously been shown to  
714 regulate several transcripts encoding genes associated with schizophrenia<sup>85</sup>. However, that study  
715 found that reducing the function of *DGCR5* lead to a reduction in the expression of its targets,  
716 again the inverse of our finding.

717 A challenge in studying psychiatric conditions has been that it is difficult to establish  
718 causal relationships between genetic variants of interest and their effects. In this study we  
719 utilized CRISPR/Cas9 to generate the 22q11.2 deletion in a control human stem cell line by  
720 inducing double strand breaks within the same repetitive elements that are normally important  
721 mediators of the deletion. While the process was relatively inefficient, we were able to obtain  
722 two independent clones that carried this large structural variant on one of the two alleles. Using  
723 these edited cells, we could then ask, without confounding by inherited variation elsewhere in the  
724 genome, which associations we had previously observed was the deletion sufficient to cause. We  
725 found that the deletion in this isogenic setting was sufficient to induce significant and aligned  
726 alterations in the expression of genes contributing to the minimal PPI network at each of the  
727 three differentiation stages, including changes, in neurons, in the activity-dependent, presynaptic,  
728 and ubiquitin/proteasome pathways as well as the heritability enrichment for schizophrenia.

729 When combined with genetic findings from 22q11.2 patients<sup>23-25</sup>, our observations lead  
730 us to a model in which the 22q11.2 deletion exerts a strong effect on genetic risk factors for  
731 NDD and ASD genes early in differentiation, while in more differentiated neurons the gene  
732 regulatory influence of the deletion shifts to risk factors for schizophrenia. Our gene editing  
733 experiments suggest that these distinct “pushes” on NDD/ASD and schizophrenia risk occur  
734 regardless of one’s genotype.

735 How exactly the 22q11.2 deletion might regulate the expression of genes outside of the  
736 deletion region remains a matter of great interest. Many studies have highlighted the role of  
737 miRNAs as possible mediators of some of the phenotypes, particularly given that *DGCR8* is  
738 located within the region. However, as discussed earlier, reduced levels of *DGCR8* would not  
739 explain our finding of reduced synaptic proteins. One intriguing possibility is that 22q11.2  
740 deletion might impact chromatin architecture, thereby regulating the expression of genes outside  
741 of the deletion region. Spatial organization of the genome has been shown to play a critical role  
742 in cell type-specific regulation of transcription<sup>86</sup>, and structural variants, such as CNVs, have  
743 been shown to alter chromatin architecture, leading to disease<sup>87</sup>. The 22q11.2 deletion lacks a  
744 large portion of chromosome 22<sup>43</sup>, which might impact chromatin organization. Indeed, a recent  
745 study using lymphoblastoid cell lines with 22q11.2 deletion revealed changes in their genome  
746 architecture<sup>88</sup>. It is thus possible that the 22q11.2 deletion spatially rearranges the genome of  
747 neuronal cells, resulting in mis-regulation of genes linked to neuropsychiatric disorders.

748 The current study is not without its limitations. Even though it is, to our knowledge, one  
749 of the largest of the effect of 22q11.2 deletion on human neuronal cells, our current sample size  
750 still falls shorts of enabling us to stratify the cohort by diagnosis, age, sex, or deletion size.  
751 Future studies with even larger sample sets could be sufficiently powered to enable the  
752 comparison of cells from 22q11.2 deletion patients with or without schizophrenia, or with or  
753 without intellectual disability or ASD, for example, to more comprehensively delineate the  
754 cellular and transcriptional changes associated with each diagnosis. It would also be interesting  
755 to stratify the cohort with respect to deletion size: while the 3Mb deletion is by far the most  
756 common, accounting for around 90% of cases, smaller nested deletions within the region still  
757 result in similar symptoms and diagnoses<sup>3,7,38,39</sup>. While the current study only includes two such

758 shorter deletions, larger studies could be better poised to identify common and distinct signatures  
759 of the distinct deletions. Other interesting co-variates to examine include donor age and sex,  
760 which do not appear to drive any of the transcriptional differences and signatures we report here  
761 but might result in subtle differences that could be detected with a larger sample set.

762 Collectively, the novel iPSC lines, CRISPR edited cell lines, RNA sequencing data and  
763 functional phenotypes we report here will provide a framework for evaluating future therapeutic  
764 targets and candidates for 22q11.2 carriers. These 22q11.2 carriers represent an interesting  
765 population for drug discovery as they are a group of individuals with more homogenous, yet still  
766 textured risk of these psychiatric illnesses. For instance, with the tools we report here, it should  
767 be possible to quantitatively address which combinations of the immediate consequences of the  
768 deletion most contribute to various components of the gene expression effects we have observed,  
769 including deficits in expression of presynaptic proteins. While these efforts are beyond the scope  
770 of our current study, we suggest that as aspects of the gene expression signal we observed are  
771 rescued, the functional relevance of such findings could be tested in the context of whether  
772 neuronal network activity is also restored in patient neurons. Through this approach, the likely  
773 multifaceted contributors to psychiatric illness that the 22q11.2 deletion confers could be  
774 quantitatively deciphered and the best approaches for alleviating its effects identified.

775

## 776 **Acknowledgements**

777 We thank the many donors, institutions and investigators world-wide that provided their cell  
778 lines and supported the publication of the results. We are indebted to Maura Charlton, Genevieve  
779 Saphier and Kristen Elwell for their assistance with the regulatory and logistical efforts required  
780 to acquire and sequence hiPSC lines. We regret the omission of any relevant references or

781 discussion due to space limitations. The Genomics Platform at the Broad Institute performed  
782 sample preparation, sequencing, and data storage. This work was funded predominantly by  
783 U01MH105669 (NIH/NIMH), with additional support from the Stanley Center for Psychiatric  
784 Research at the Broad Institute, R37NS083524 and U01MH115727. RN was also supported by a  
785 NARSAD young investigator award (Brain and Behavior Research Foundation) and a Bn10  
786 grant (Broad Institute), and OP was also supported by the Sigrid Juselius Foundation, Orion  
787 Research Foundation, Instrumentarium Science Foundation, and Päivikki and Sakari Sohlberg  
788 Foundation.

789

## 790 **Data Availability Statement**

791 The raw sequence datasets generated during the current study are not currently publicly available  
792 due to patient confidentiality and multiple different consents of population cohorts used but  
793 subsets of the data are available from the corresponding authors on reasonable request. Computer  
794 code relevant to the PPI analysis has been deposited in GitHub  
795 (<https://github.com/alexloboda/PPIttools>). Other computer code and data analysis will be made  
796 available upon request.

797

## 798 **Author contributions**

799 R.N., O.P. and K.E. conceived the work, designed the experiments, analyzed the data and wrote  
800 the manuscript. R.N. supervised and performed the experiments, with help from A.T., C.B.,  
801 M.T., R.M., E.J.G., V.V., D.H., E.P., and E.Z. O.P. performed the computational analysis, with  
802 help from M.T. and G.G. M.A. performed the PPI analysis, with help from A.L. and supervision  
803 from M.D. C.B. performed the proteomics experiments with help from J.A.P. and supervision

804 from J.W.H. A.G. carried out the SNP heritability analysis, with oversight from B.N. T.S. carried  
805 out the rare variant analysis. J.S. performed the MEA analysis. D.M., A.B., A.M.B. and D.Z.H.  
806 carried out the CRISPR editing, supervised by L.E.B. A.N. and C.L. assisted with stem cell  
807 compliance and data deposition. O.K., E.H., and M.K. provided the NFID cell lines, with  
808 oversight from A.P. C.M.H. and A.K.K. contributed the KI cell lines. B.C. and D.M. provided  
809 cell lines from Mclean Hospital. J.M., R.A. provided the Umea samples, R.D. provided the  
810 Stanford cell lines, and R.P. provided the MGH cell line. S.M. and S.H. provided guidance  
811 throughout the project.

812

813 **Competing interests**

814 K.E. is Group Vice President, Head of Research and Early Development at Biogen  
815 Pharmaceuticals and a founder of Q-state Biosciences, Quralis and Enclear. J.W.H. is a founder  
816 and advisor of Caraway Therapeutics.

817

818

819

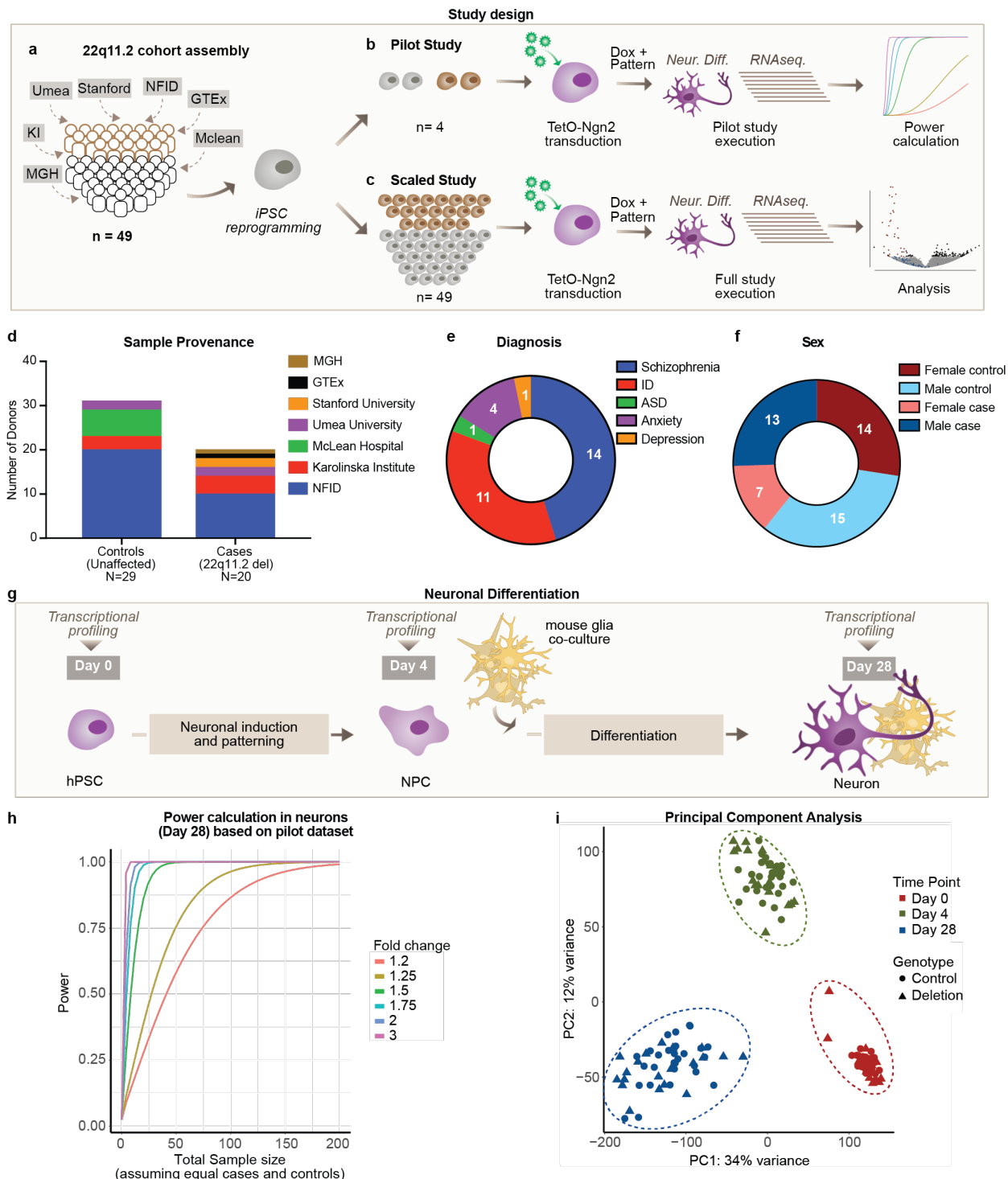


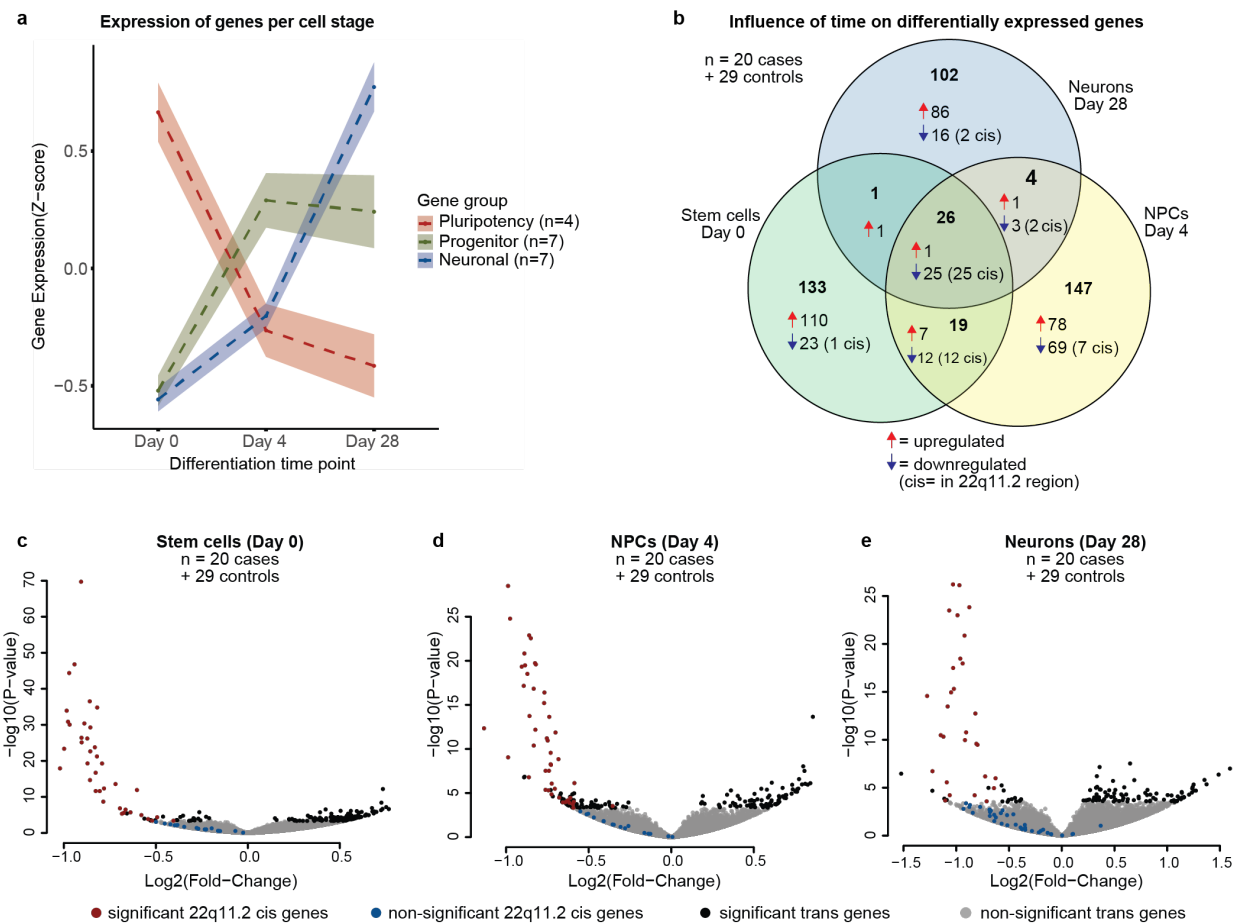
**Fig. 1. Design of a statistically powered study to determine the impact of 22q11.2 deletion on gene expression.** **a**, Final sample set composed of 20 cell lines with 22q11.2 deletion (brown) and 29 controls (grey), collected at seven locations (MGH: Massachusetts General Hospital, KI: Karolinska Institute, Umeå: Umeå University, NFID: Northern Finnish Intellectual Disability Cohort (Institute for Molecular Medicine Finland), GTEX: Genotype-Tissue Expression Project, McLean: McLean Hospital) **b**, Pilot study using four hiPSC lines differentiated into neurons through transduction with TetO-Ngn2, Ub-rtTA and TetO-GFP lentivirus and subjected to RNA sequencing. RNA abundances were then used to estimate the appropriate sample size for differential gene expression for the final study. **c**, The final dataset consisted of 49 cell lines that were differentiated and subjected to RNA sequencing. **d**, Provenance **e**, Diagnosis and **f**, Sex of the samples in the final cohort. **g**, Neuronal differentiation protocol, previously published and characterized<sup>34,37</sup> consisting of the combination of Ngn2 overexpression with

820  
821  
822  
823  
824  
825  
826  
827  
828  
829

830 forebrain patterning using small molecules (SB431542, LDN193189 and XAV939). Samples were harvested for RNA  
831 sequencing at the stem cell (day 0), neuronal progenitor cell (NPCs) (day 4) and neuronal (day 28) stages. **h**, Power estimation in  
832 the pilot dataset for median expressed genes (24 read counts) for different fold-changes and sample sizes in neurons. **i**, Principal  
833 component analysis (PCA) of RNA sequencing data from the full study.  
834

835

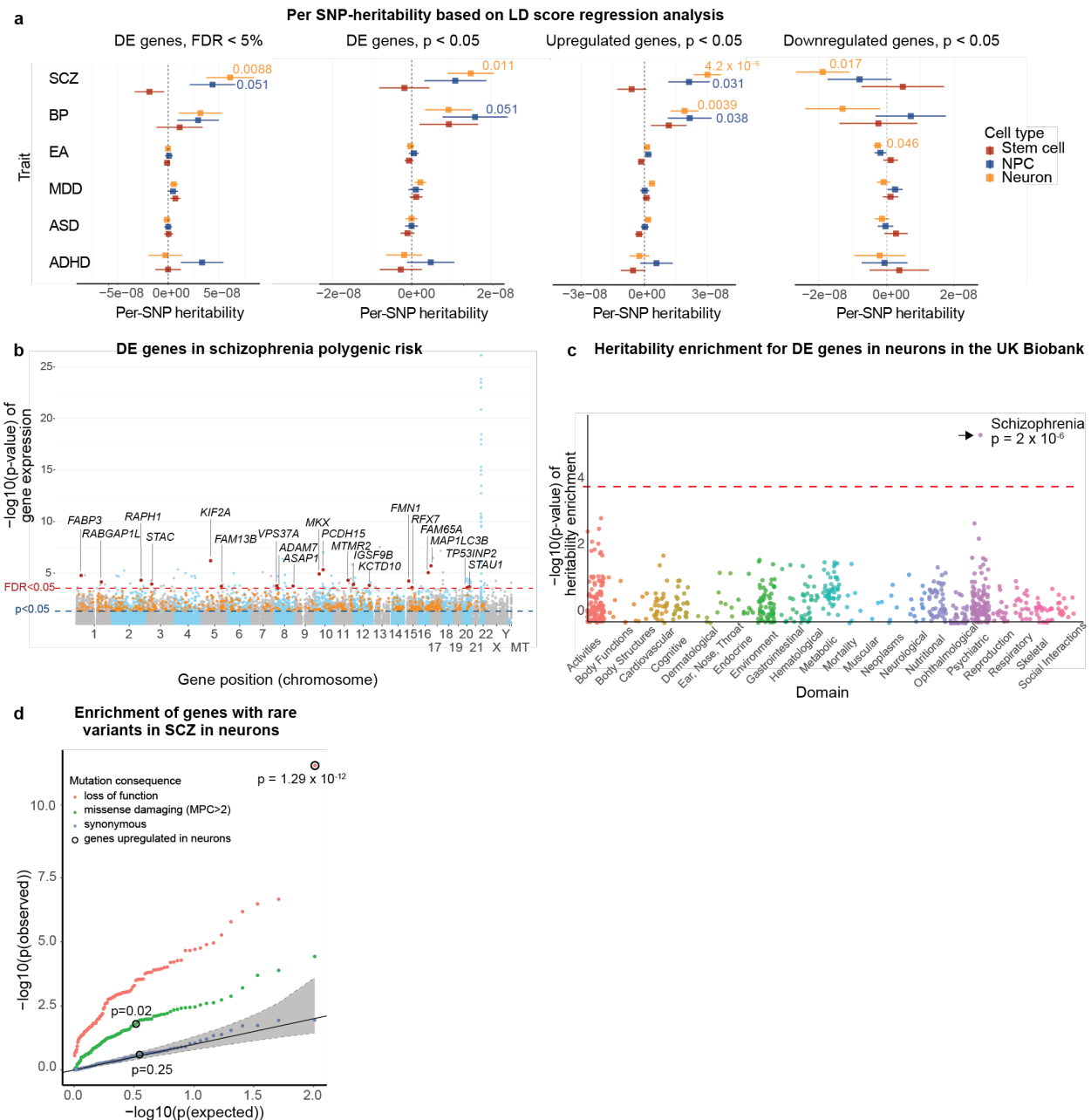
836



837  
838  
839  
840  
841  
842  
843  
844  
845  
846  
847  
848  
849

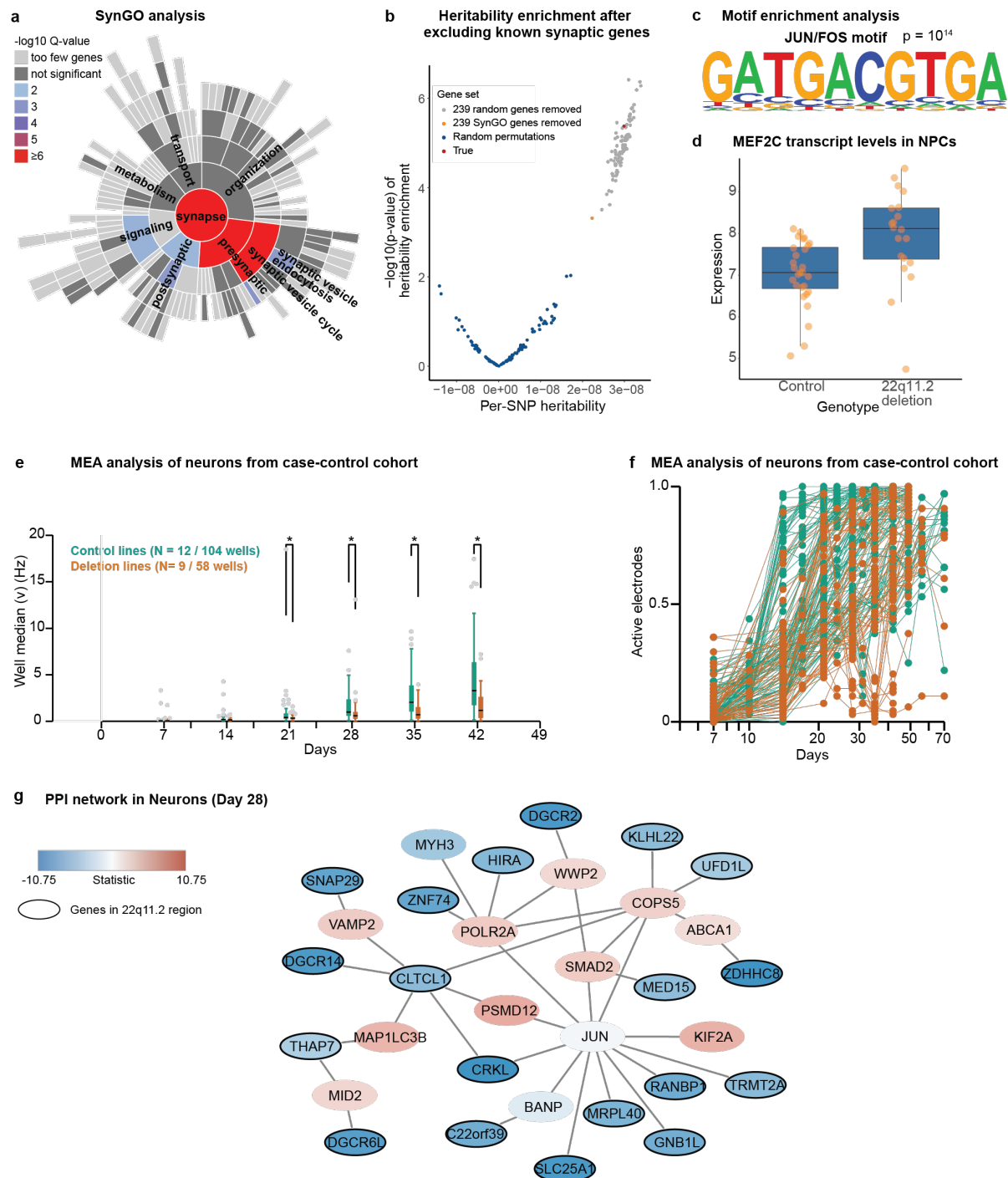
850

**Fig. 2. Cell-type specific effects of the 22q11.2 deletion.** **a**, Expression of selected marker genes for defined specific cell stages by suppression of genes related to pluripotency (*SOX2*, *OCT4*, *NANOG*, *MKI67*) and up-regulation of genes characteristic for neural progenitor cells (*NEUROD1*, *SOX2*, *EMX2*, *OTX2*, *HES1*, *MSII*, *MKI67*) and mature neurons (*NEUN*, *SYN1*, *DCX*, *MAP2*, *TUJ1*, *NCAM*, *MAPT*) as the differentiation progresses (gene lists also provided in Extended Data Fig. 2c). **b**, Venn Diagramm highlighting the number and directionality of shared and unique differentially expressed genes between deletion carriers and controls at each cell stage. Genes within the deletion region (cis) are mostly shared across development stages, whereas genes outside the deletion region (trans) are cell-stage specific. **c-e**, Volcano plots showing differential gene expression in stem cells (c), NPCs (d) and neurons (e). Significantly differentially expressed genes (FDR<5%) within the deletion region are presented in red and outside deletion in black. Non-significant genes in deletion region are presented in blue.



851

852 **Fig. 3. Heritability enrichment for schizophrenia risk genes 22q11.2 deletion neurons.** **a**, Marginal enrichment in per-SNP  
 853 heritability explained by common (MAF > 5%) variants within 100kb of genes differentially expressed, estimated by LD Score  
 854 regression. Six traits were analyzed: SCZ=schizophrenia, BP=bipolar disorder, EA=educational attainment, MDD=major  
 855 depressive disorder, ASD=autism spectrum disorder, ADHD=attention deficit hyperactivity disorder, at all three cell stages,  
 856 showing enrichment for schizophrenia most prominently in genes upregulated in 22q11.2 deletion neurons. DE=differentially  
 857 expressed. Four groups of DE genes were analyzed. Right, all DE genes with an FDR < 5%. Middle right, all nominally  
 858 significant DE genes (p<0.05). Middle left, all nominally significant upregulated DE genes (p<0.05). Left, all nominally  
 859 significant downregulated DE genes (p<0.05). **b**, DE genes in 22q11.2 neurons with nominally significant gene-wise association  
 860 to schizophrenia from MAGMA ( $p_g < 0.05$ ). **c**, GWAS summary statistics for 650 traits from the UK-biobank showing significant  
 861 enrichment for heritability only for schizophrenia ( $p=2 \times 10^{-6}$ ) in genes upregulated in deletion neurons. **d**, qq plot of p-values for  
 862 the enrichment of rare coding LoF, missense damaging or synonymous variants in schizophrenia patients in genes upregulated in  
 863 deletion neurons (circled in black) and 100 random gene sets matched by expression level to the upregulated genes.



864  
865  
866  
867  
868  
869  
870  
871  
872  
873

**Fig. 4. Impact of the 22q11.2 deletion on synaptic gene expression and network activity.** **a**, SynGO annotation for genes upregulated in neurons showing enrichment for synaptic processes. **b**, Heritability enrichment for schizophrenia after excluding the 239 genes with SynGO annotation. **c**, Motif Enrichment analysis in upregulated genes ( $p < 0.05$ ), showing enrichment of JUN / FOS targets. **d**, *MEF2C* is upregulated in NPC of 22q11.2 deletion carriers. **e**, Spike count (mean number of spikes in a 10 second period). The activity of neurons derived from control (green,  $N = 12$  lines, 104 wells) is compared to neurons from cases with 22q11.2 deletion ( $N = 9$  lines, 54 wells). **f**, Proportion of electrodes detecting spontaneous activity, against the number of days post-induction. **g**, The most weighted sub-cluster graph for protein-protein interactions (PPI) for differentially expressed genes in neurons.

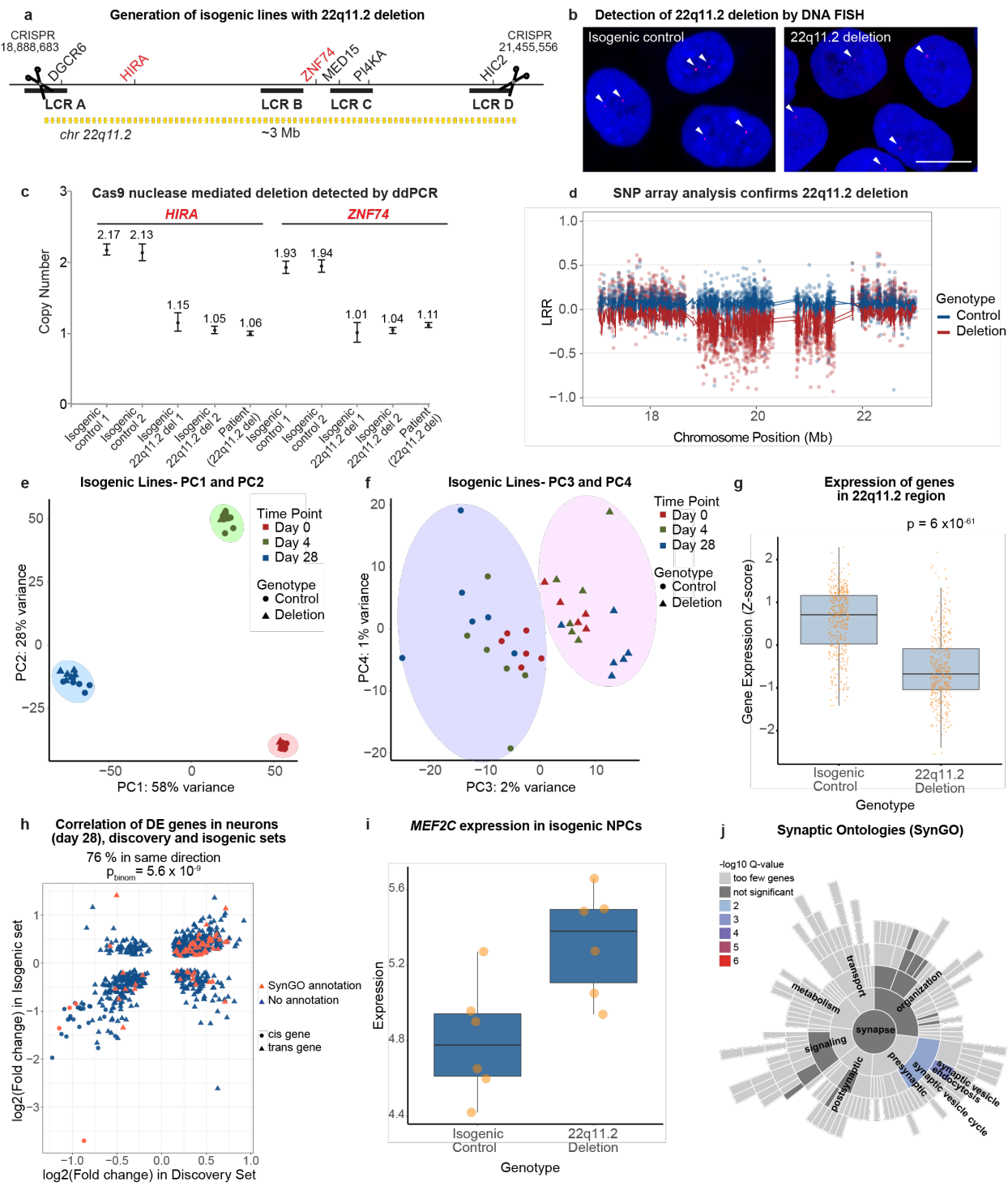
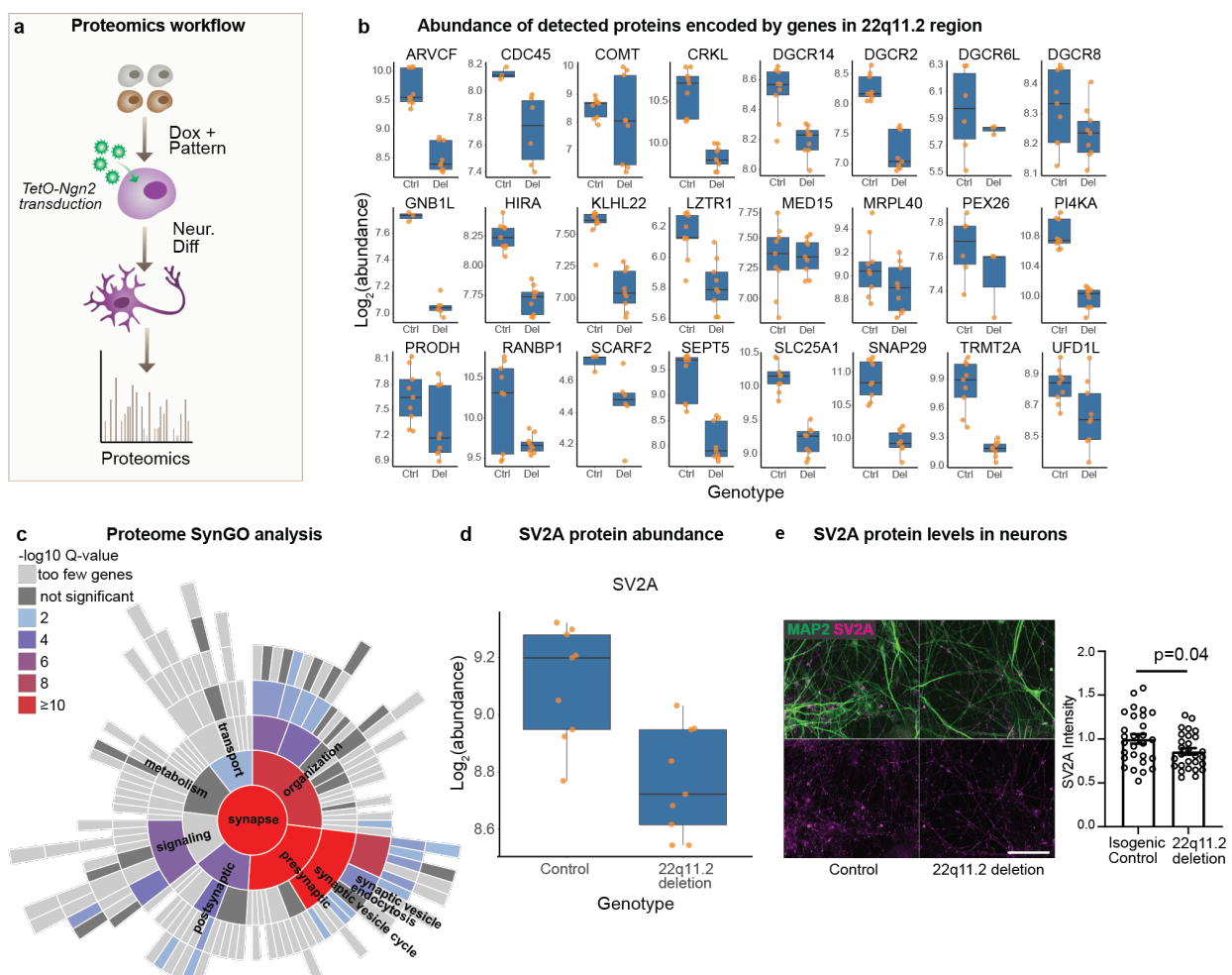


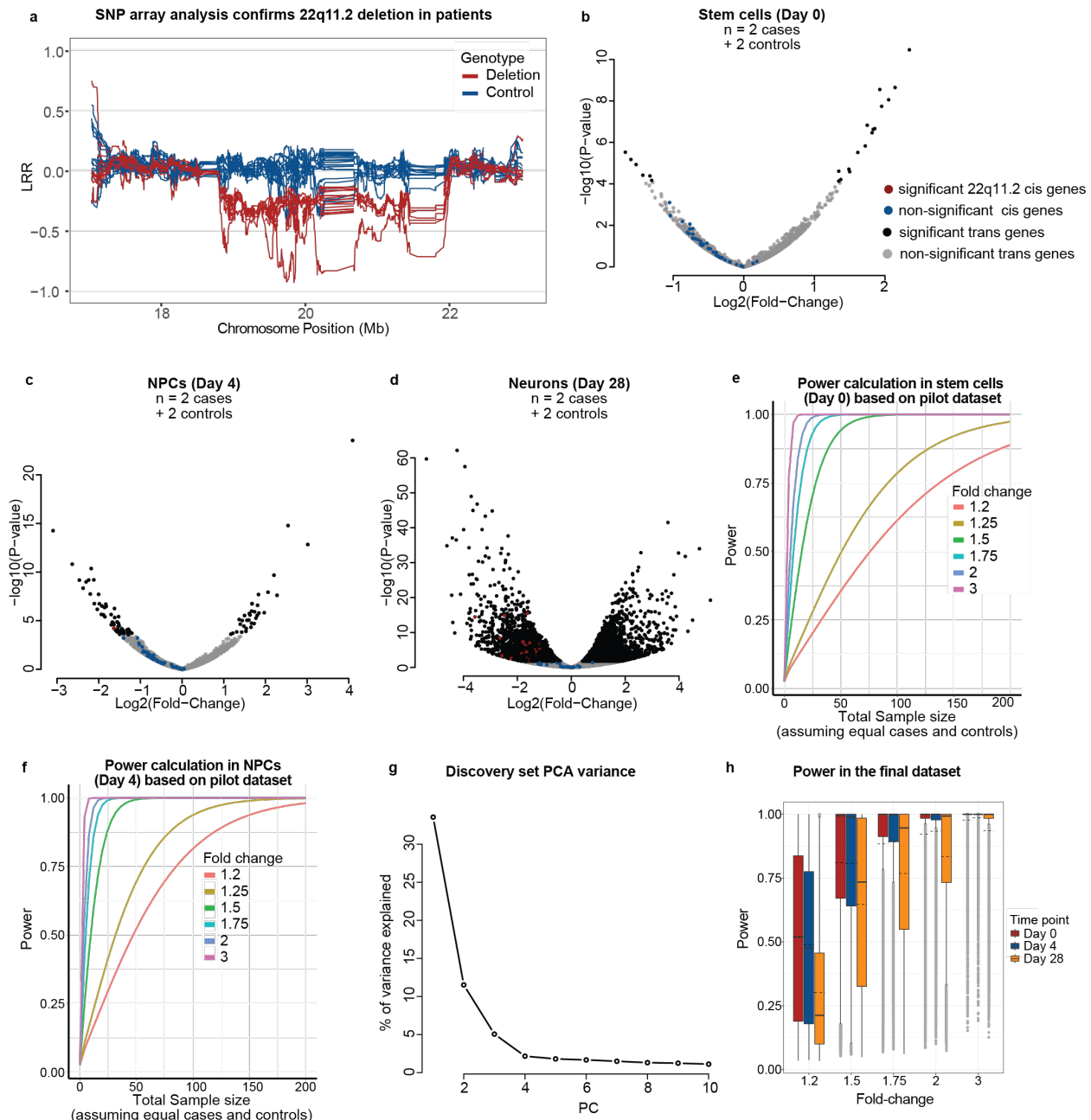
**Fig. 5. Validation of causality between the differentially expressed genes and the deletion genotype in an isogenic setting.**

**a**, Generation of isogenic lines with 22q11.2 deletion using CRISPR Cas9 guide RNAs that cut within the low copy repeats (LCRs) flanking the 3Mb 22q11.2 deletion. The coordinates for the genomic position of the CRISPR guides on chromosome 22 are indicated (Hg19). **b**, Detection of isogenic 22q11.2 deletion using DNA FISH analysis and a probe generated probe using CTD-2300P14 (Thermo Fisher Scientific, Supplier Item: 96012). Blue = DAPI (DNA), Red=22q11.2 region. Scale bar: 10um. **c**, ddPCR assay to determine the copy numbers of the HIRA and ZNF74 genes, located in the 22q11.2 region, to validate isogenic deletion of 22q11.2. **d**, SNP array marker intensity (LRR) for SNPs overlapping the deletion locus confirms isogenic 22q11.2 deletion in two clones (red). **e,f**, Principal component analysis of cell lines with and without isogenic 22q11.2 deletion. Circles =

884 genes within the 22q11.2 interval (cis). Triangles = genes outside 22q11.2 (trans). **e**, PC1 and PC2 separate cells by  
 885 developmental stage. **f**, PC3 and PC4 separate cells by deletion genotype. **g**, Significant downregulation of genes in 22q11.2  
 886 region in lines with isogenic 22q11.2 deletion. **h**, Correlation of fold changes in differentially expressed genes in discovery and  
 887 isogenic datasets in neurons. 32 genes were detected and significantly changed in transcript levels in the discovery cohort and the  
 888 isogenic lines (adjusted p-value < 0.05 in both experiments), of which nine were located outside the deletion region (*FAM13B*,  
 889 *KMT2C*, *HYAL2*, *DNPH1*, *ZMYM2*, *VAPB*, *SMG1*, *CPSF4*, *MAP3K2*) and the rest were in cis. All 32 genes were changed in the  
 890 same direction both in the discovery and isogenic cohorts ( $p = 0.004$ , binomial test). Genes with a SynGO annotation are shown  
 891 in red, genes with no SynGO annotation are shown in blue. Circles = cis genes. Triangles = trans genes. **i**, *MEF2C* is upregulated  
 892 in NPCs of deletion carriers compared to isogenic controls, similar to the discovery dataset. **j**, SynGo annotation of genes  
 893 induced in isogenic neurons with 22q11.2 deletion showing enrichment for synaptic vesicle cycle and endocytosis.  
 894  
 895  
 896  
 897  
 898



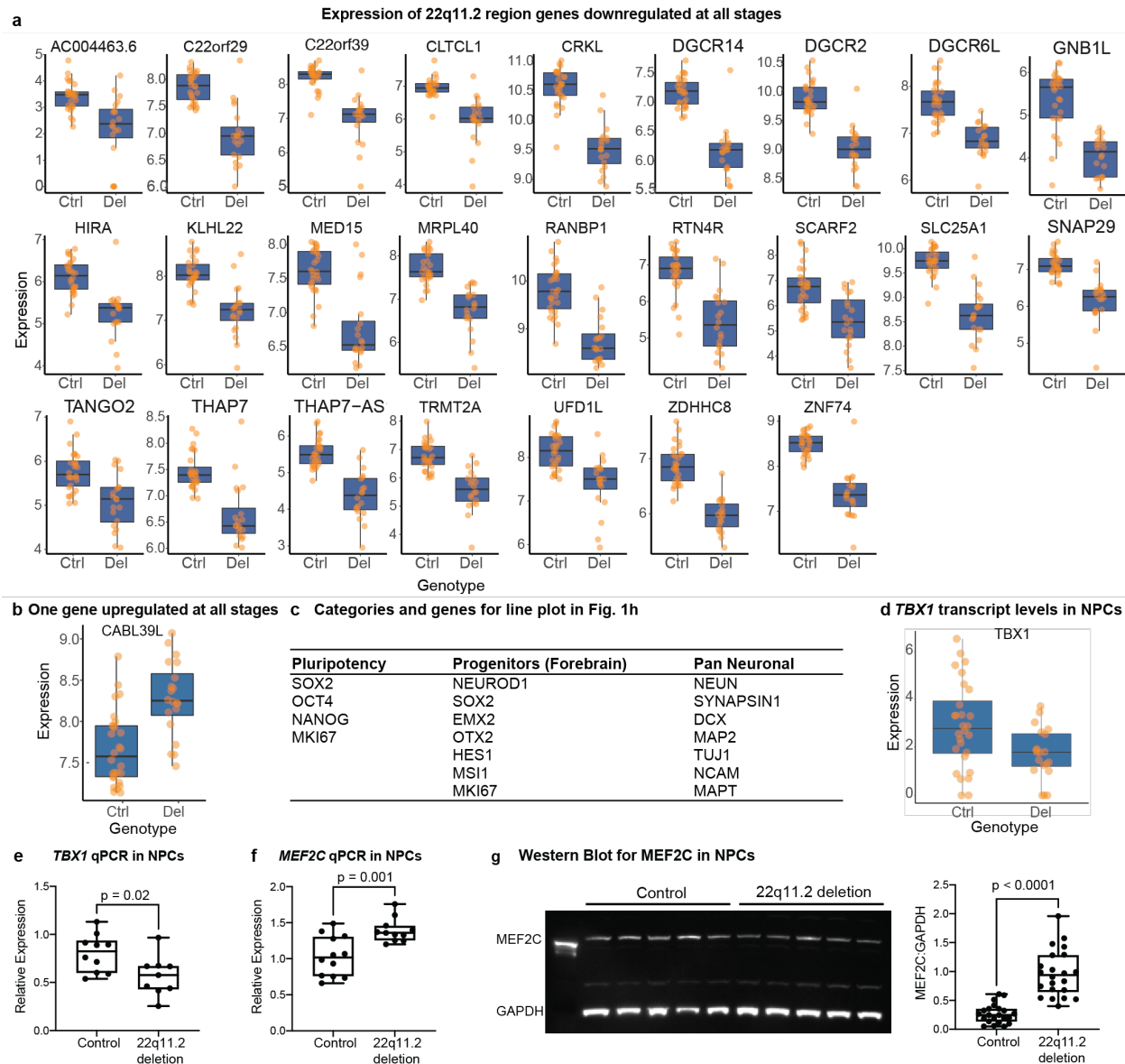
899  
 900  
 901 **Fig. 6. Whole cell proteomics on 22q11.2 deletion neurons.** **a**, Workflow schematic. Neurons from deletion carriers and  
 902 controls were harvested 28 days post neuronal induction. **b**, Abundance of proteins encoded by genes in the 22q11.2 region  
 903 detected by proteomics in neurons. Del = 22q11.2 deletion. Ctrl = control. **c**, Synaptic gene ontologies (SynGO) in proteins  
 904 downregulated in deletion carrier neurons. **d**, SV2A protein levels detected by proteomics are decreased in deletion carrier  
 905 neurons. **e**, SV2A protein levels detected by antibody staining are decreased in day 28 neurons derived from isogenic lines with  
 906 22q11.2 heterozygous deletion compared to controls. (Left) Representative confocal images of control and 22q11.2 deletion  
 907 neurons stained with antibodies against SV2A (magenta) and MAP2 (green). Scale bar = 100 μm. (Right) Quantification of total  
 908 SV2A fluorescence within MAP2-positive neurites normalized to isogenic controls. Data are means  $\pm$  SEM. Individual points are  
 909 analyzed fields of view from 4 independent inductions per condition. Statistical analysis by Student's t test reveals statistically  
 910 significant ( $p=0.037$ ) decrease in SV2A levels in deletion neurons.



911

912 **Extended Data Fig. 1. Discovery and pilot datasets.** **a**, Validation of the full-size deletion in 22q11.2 lines used in the current  
 913 study by sliding-window average of SNP marker intensity (LRR) in the deletion locus. **b-d**, Volcano plots showing differentially  
 914 expressed genes in the pilot dataset. **e**, Power estimation in the pilot dataset for median expressed genes for different fold-changes  
 915 and sample sizes in stem cells. **f**, Power estimation in the pilot data set for median expressed genes for different fold-changes and  
 916 sample sizes in neuronal progenitor cells (NPCs). **g**, Variance explained by the first 10 principal components in the discovery  
 917 sample. **h**, Estimated power in the final (discovery) dataset, at each time point.

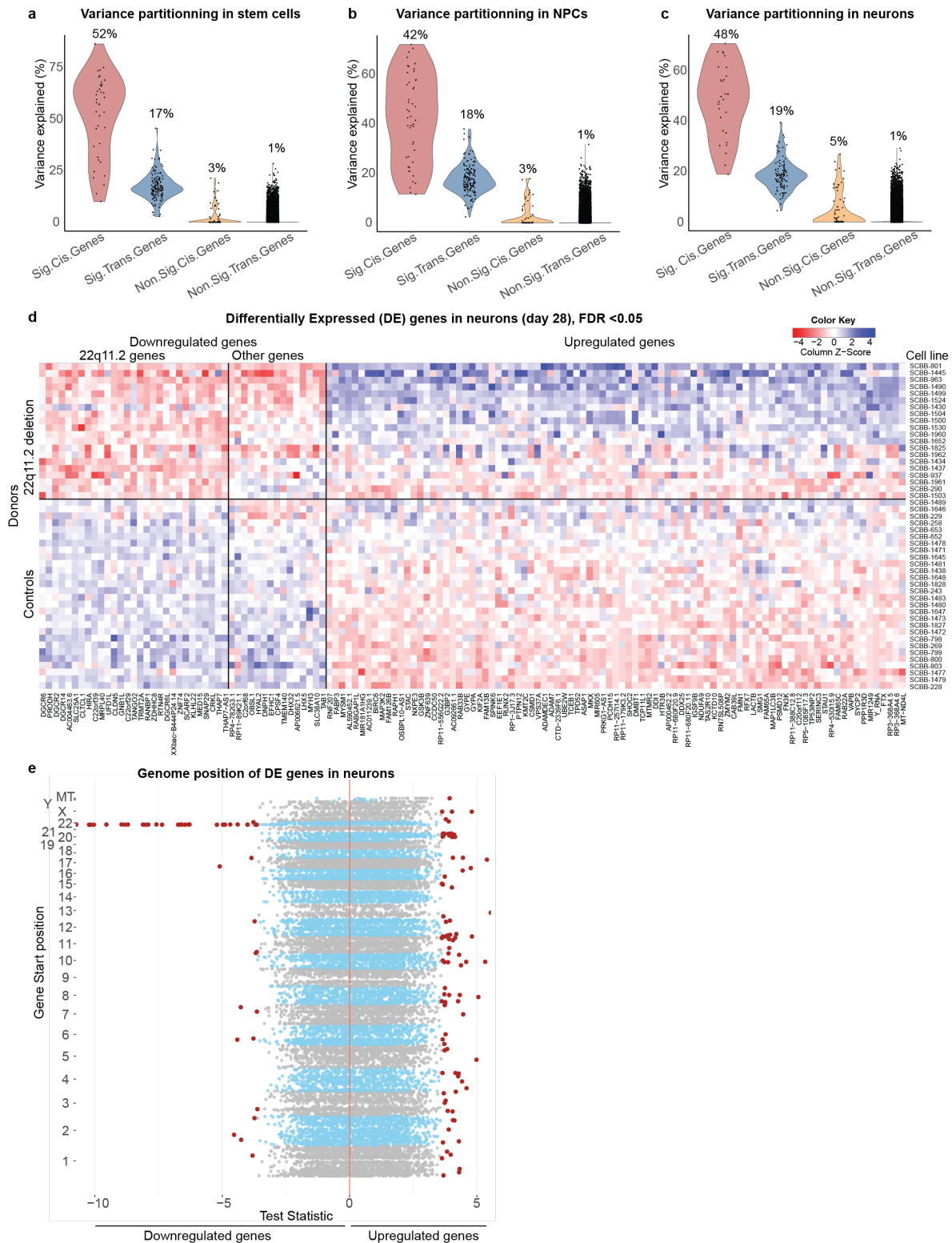
918



920 **Extended Data Fig. 2. Expression of differentially regulated genes.** **a**, Expression of significant cis genes shared across all  
 921 three developmental stages. **b**, *CAB39L* is the only trans gene upregulated in all developmental stages. **c**, List of categories and  
 922 genes used in Fig. 2a. **d**, *TBX1* is downregulated in NPC of 22q11.2 deletion carriers. **e**, Relative expression of *TBX1* via qPCR in  
 923 Day 4 NPCs from control and 22q11.2 deletion patients (Samples: 3/3, 2BR/2TR,  $p < 0.05$ ). **f**, Relative expression of *MEF2C* via  
 924 qPCR in NPCs from control and patients (Samples: 3/3, 2BR/2TR,  $p < 0.01$ ). **g**, Expression of *MEF2C* in total protein lysates from  
 925 control and 22q11.2 deletion NPCs. (Left) Total protein lysates from control (left five lanes) and deletion lines (right five lanes)  
 926 probed for *MEF2C* (top) and *GAPDH* (bottom). (Right) Statistical analysis by Student's t test reveals statistically significant  
 927 decrease in *MEF2C* expression in the deletion lines. (Samples: 5/5, 1BR/3TR,  $p < 0.0001$ ). BR = biological replicate (independent  
 928 differentiations); TR = technical replicate (independent wells).  
 929

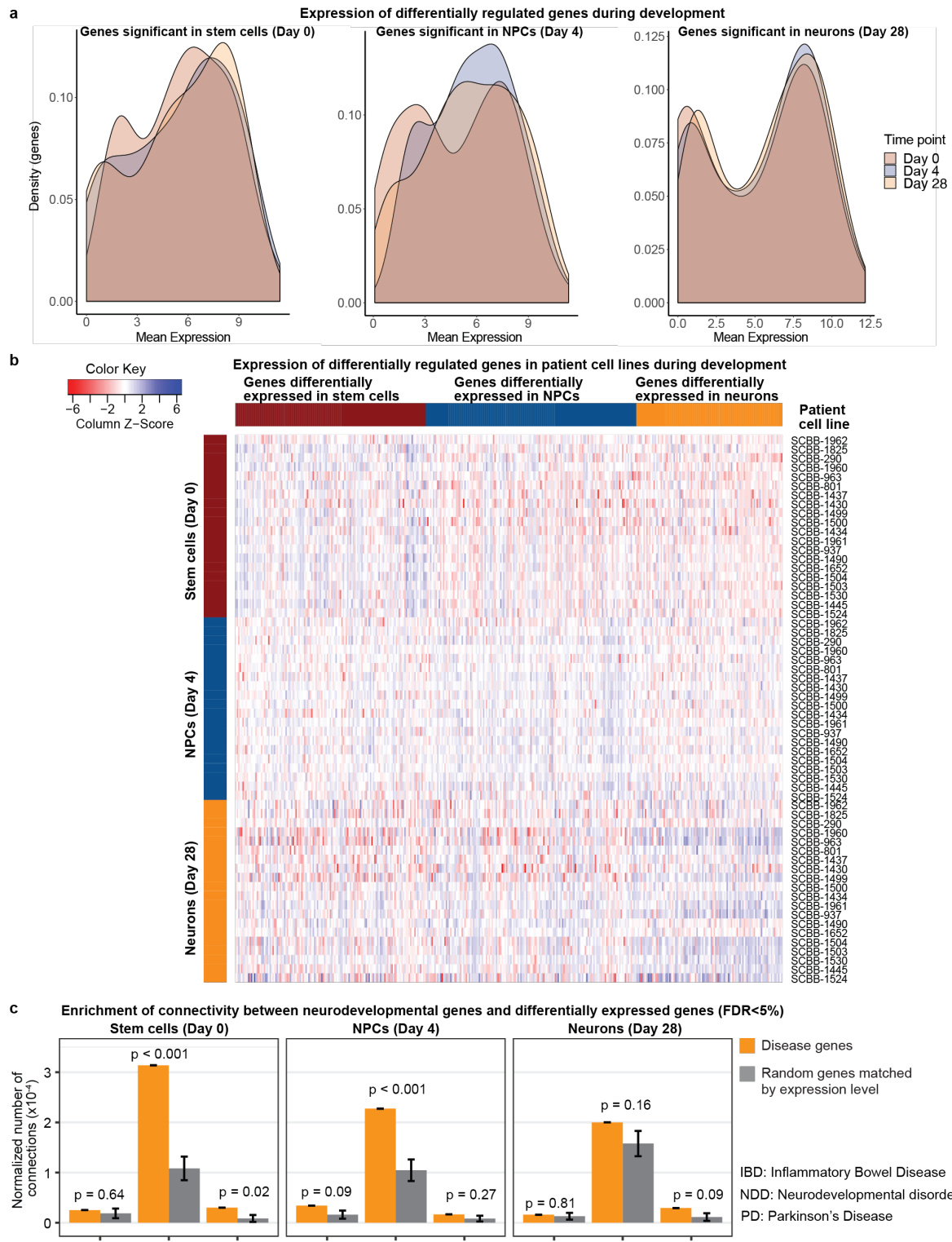
930

931

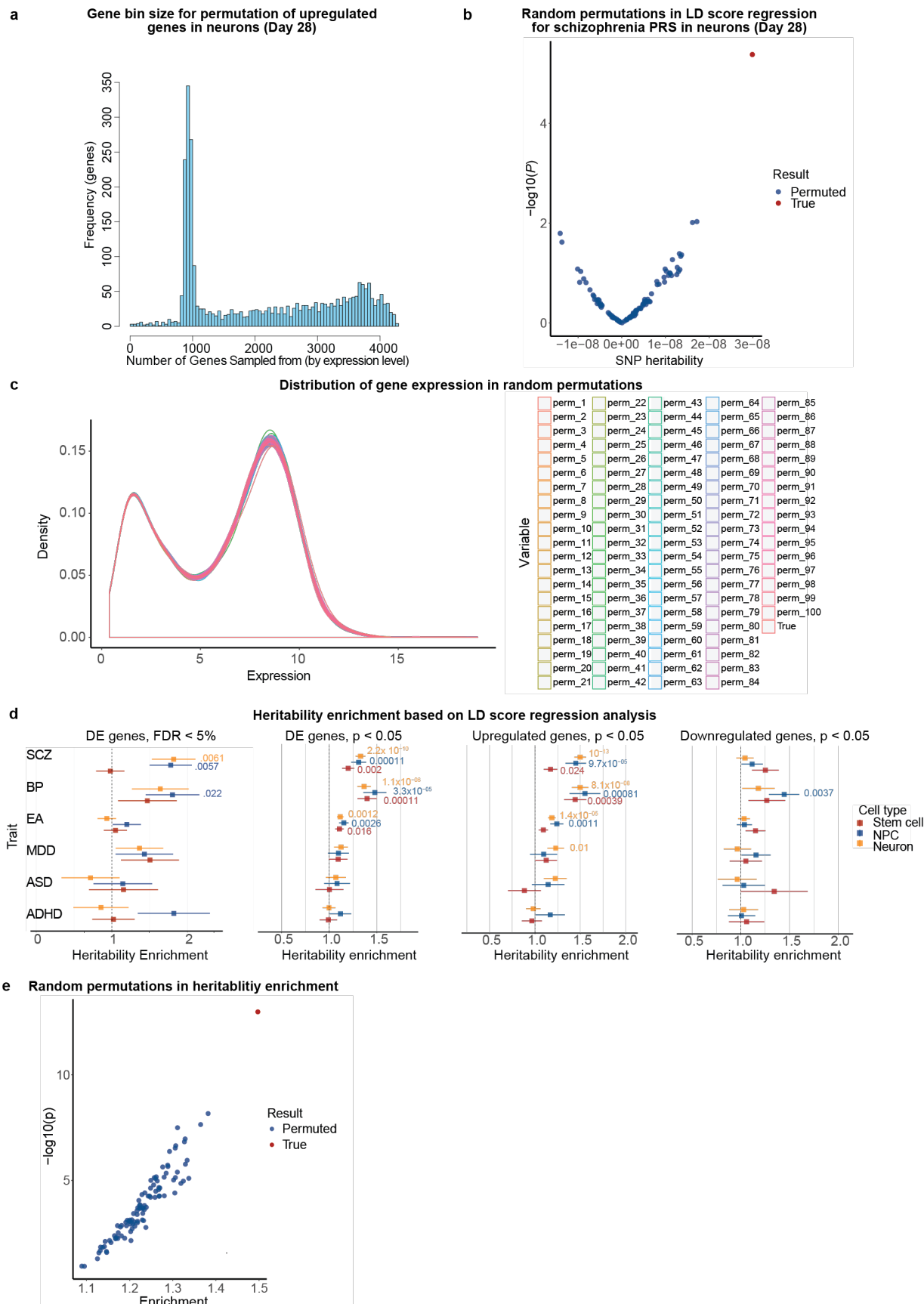


932  
933

934 **Extended Data Fig. 3. Variance partitioning and expression of differentially regulated genes** **a-c**, Variance in gene  
935 expression explained by the deletion genotype in different gene categories in the final dataset in **a**, Stem cells, **b**, Neuronal  
936 progenitor cells and **c**, Neurons. **d**, Heatmap of 133 genes differentially expressed in neurons showing the range of expression, in  
937 all donor lines, of genes down or upregulated. **e**, Test statistic for differential expression plotted by chromosomal position of  
938 differentially expressed genes in cells with 22q11.2 deletion. Differentially expressed genes (FDR<5%) are colored in red.

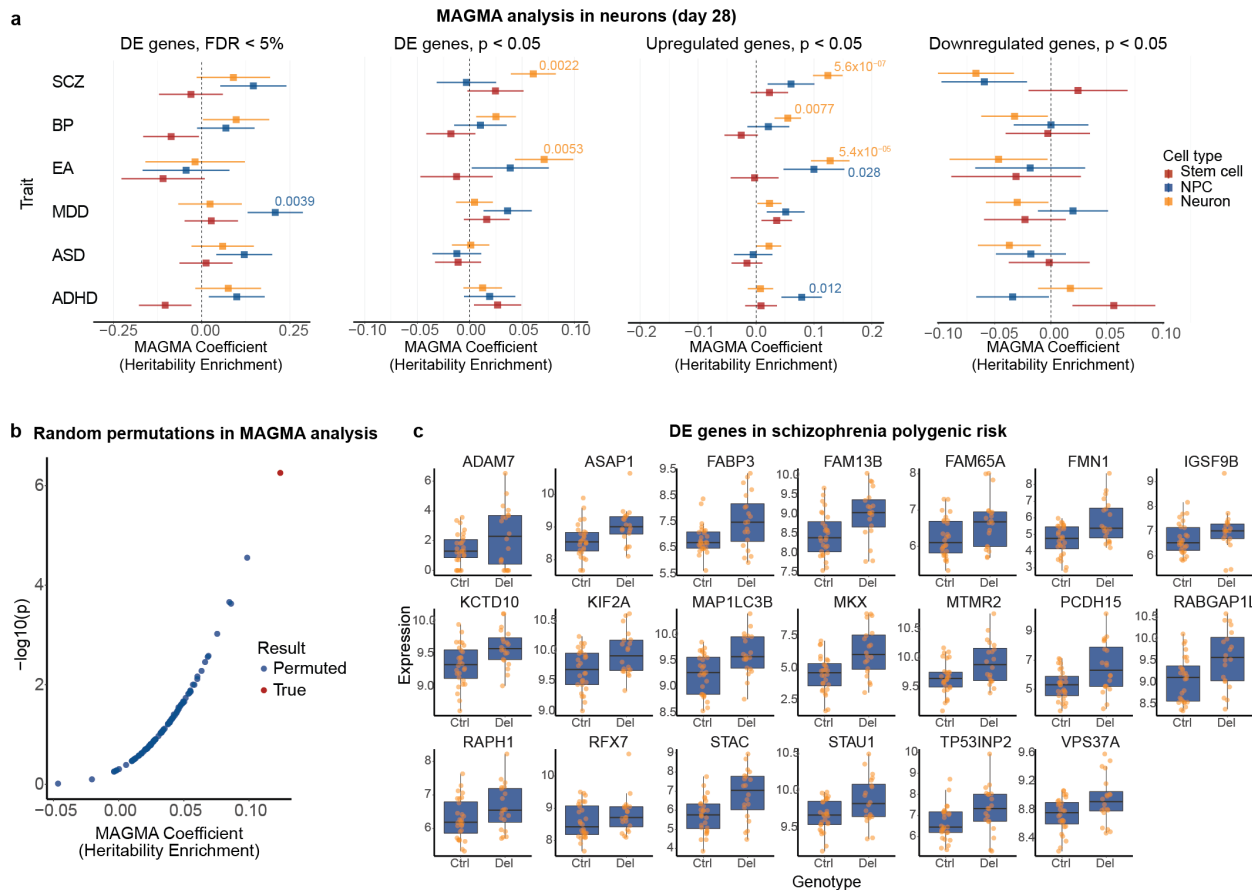


**Extended Data Fig. 4. Expression of genes differentially regulated at specific cell stages in 22q11.2 deletion cells across developmental stages.** **a**, density plots and **b**, heatmap showing that the differentially regulated genes are expressed at similar levels across all three cell stages. **c**, Connectivity enrichment analysis. Enrichment of interactors of proteins encoded by genes associated with intellectual disability and autism (NDD) and differentially expressed genes ( $FDR < 5\%$ ) in the early developmental stages after 1000 random permutations. Gene products encoded by genes linked to inflammatory bowel disease (IBD) yielded no enrichment for protein-protein interactions between the differentially expressed genes at any cell stage, and genes linked to Parkinson's disease (PD) yielded no enrichment in NPCs or neurons.



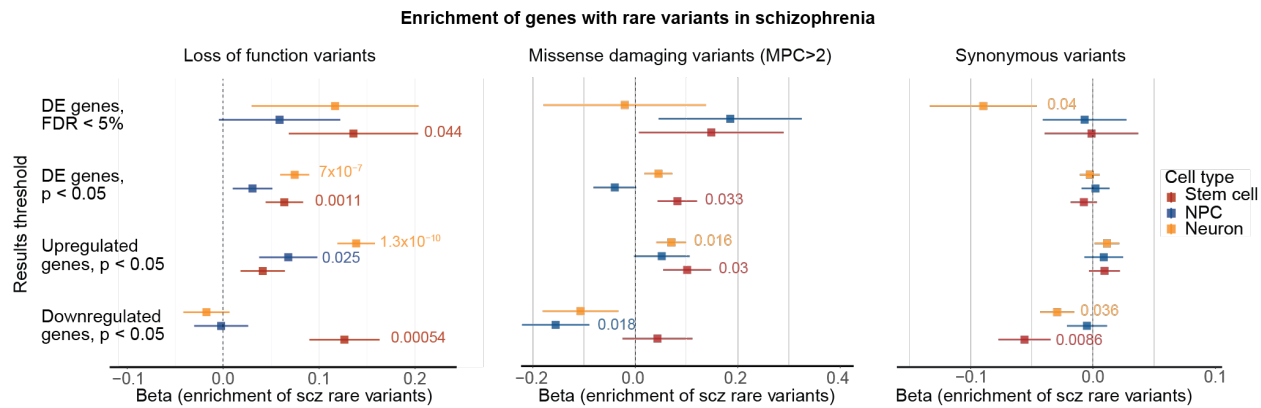
948 **Extended Data Fig. 5. LD-score regression analysis.** **a**, Gene bin size for permutation of upregulated genes in neurons. **b**, Per-  
 949 SNP heritability enrichment in LD score regression for random permutations (in blue) and the upregulated genes (in red) in  
 950 neurons **c**, Distribution of gene expression in random generated gene sets in the 100 permutations for per-SNP heritability. **d**,  
 951 Heritability enrichment analysis of six traits across the three developmental cell stages. SCZ= schizophrenia, BP=bipolar  
 952 disorder, EA= educational attainment, MDD= major depressive disorder, ASD= autism spectrum disorder, ADHD=attention  
 953 deficit hyperactivity disorder. **e**, LD score regression heritability enrichment in random expression matched gene lists from 100  
 954 permutations (in blue) compared to the up-regulated genes in neurons (in red).  
 955

956

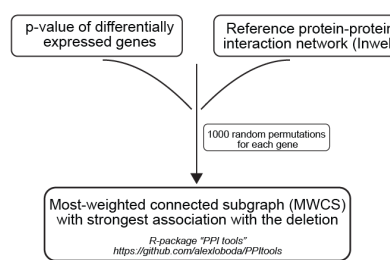


957

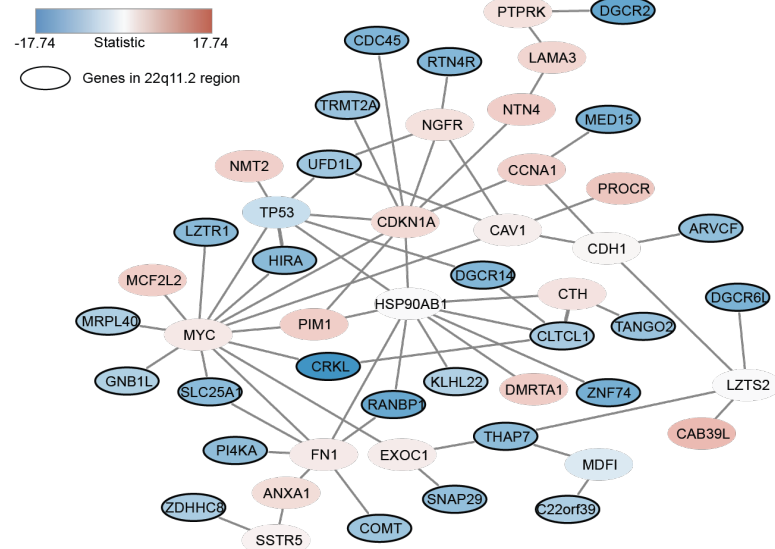
958 **Extended Data Fig. 6. MAGMA (Multi-marker Analysis of GenoMic Annotation) analysis in neurons.** **a**, MAGMA  
 959 heritability enrichment analysis of six traits across the three developmental cell stages. SCZ= schizophrenia, BP=bipolar disorder,  
 960 EA= educational attainment, MDD= major depressive disorder, ASD= autism spectrum disorder, ADHD=attention deficit  
 961 hyperactivity disorder. **b**, Magma heritability enrichment in random expression matched gene lists from 100 permutations (in  
 962 blue) compared to the up-regulated genes in neurons (in red). **c**, Expression of the differentially expressed genes contributing to  
 963 the MAGMA schizophrenia signal (FDR <5%).



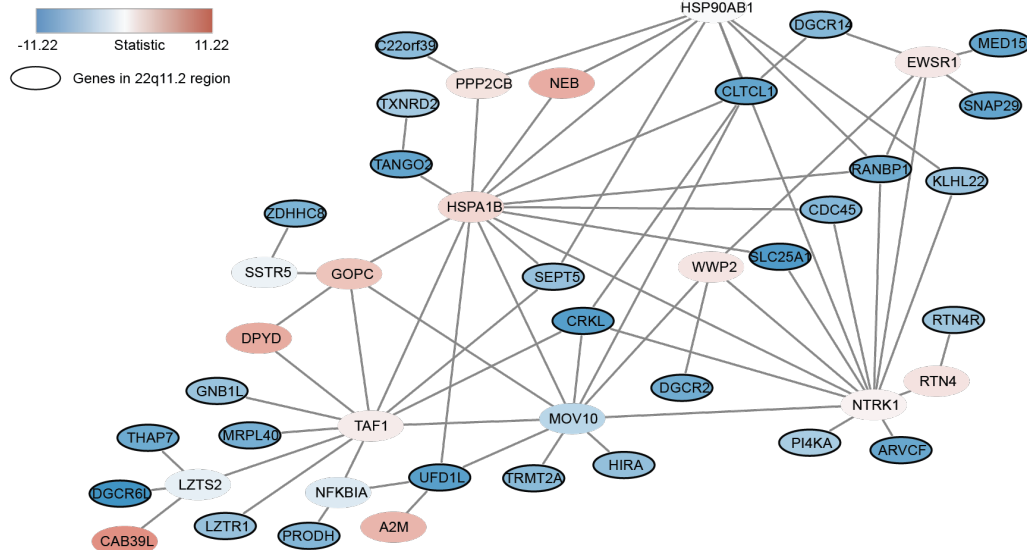
**a Protein-protein interaction network analysis workflow**



**b PPI network in Stem Cells (Day 0)**



**c PPI network in NPCs (Day 4)**



969

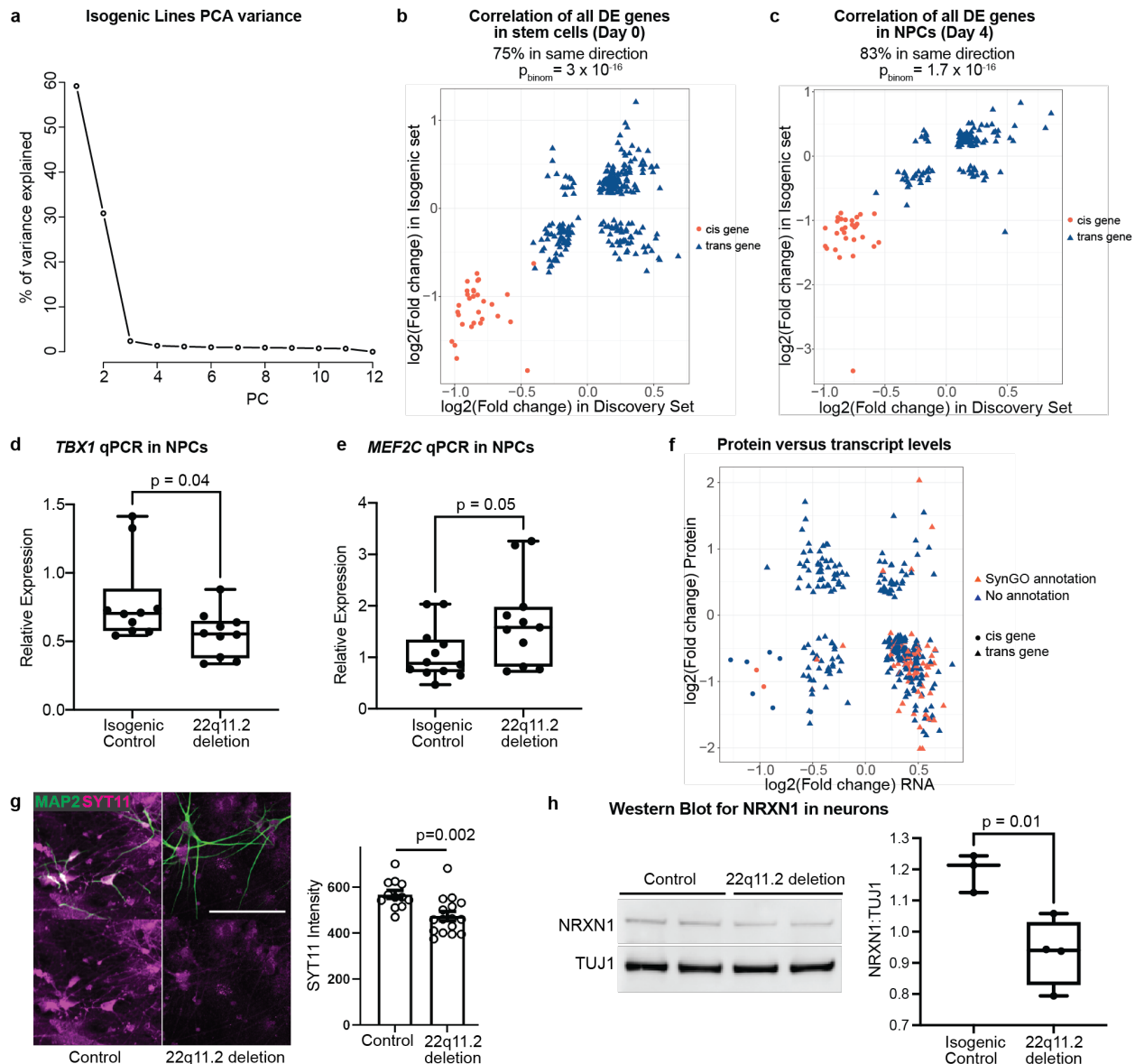
970

971

972

973

**Extended Data Fig. 8. The most weighted sub-cluster graph for protein-protein interactions (PPI) for differentially expressed genes. a, Workflow. b, Network in Stem cells. c, Network in neuronal progenitor cells.**



974

975 **Extended Data Fig. 9. Isogenic line and protein analysis.** **a**, Variance explained by each principal component from RNA  
 976 sequence data in the isogenic lines. **b-c**, Correlation of fold-changes of differentially expressed genes in discovery and isogenic  
 977 datasets in stem cells (**b**) and neuronal progenitors (**c**). Red circles = cis genes. Blue triangles = trans genes. **d**, Relative  
 978 expression of TBX1 via qPCR in Day 4 NPCs from isogenic control and 22q11.2 deletion lines (Samples: 2/2, 3BR/2TR,  
 979  $p=0.04$ ). **e**, Relative expression of MEF2C via qPCR in Day 4 NPCs from isogenic control and 22q11.2 deletion lines (Samples:  
 980 2/2, 3BR/2TR,  $p=0.05$ ). **f**, Protein versus RNA levels of genes differentially expressed in 22q11.2 deletion carrier patient  
 981 neurons. Genes with a SynGO annotation are shown in red, genes with no SynGO annotation are shown in blue. Circles = cis  
 982 genes. Triangles = trans genes. **g**, Synaptotagmin-11 (SYT11) protein levels are decreased in Day 28 22q11.2 deletion neurons.  
 983 (Left) Representative confocal images of control and 22q11.2 deletion patient neurons stained with antibodies against SYT11  
 984 (magenta) and MAP2 (green). Scale bar is 100  $\mu$ m. (Right) Quantification of total SYT11 fluorescence within MAP2-positive  
 985 area normalized to controls. Data are represented as means  $\pm$  SEM. Individual points are analyzed fields of view from 3  
 986 independent control lines and 4 patient-derived lines. Statistical analysis by Student's t test reveals statistically significant  
 987 ( $p=0.0022$ ) decrease in SYT11 levels in patient-derived neurons. **h**, Expression of Neurexin-1 (NRXN1) in total protein lysates  
 988 from isogenic control and 22q11.2 deletion neurons. (Left) Total protein lysates from isogenic control (left two lanes) and  
 989 deletion lines (right two lanes) stained for NRXN1 (top) and TUJ1 (bottom). (Right) Statistical analysis by Student's t test reveals  
 990 statistically significant decrease in Neurexin-1 expression in the deletion lines. (Samples: 5/5, 2BR/2TR,  $p=0.01$ ). BR =  
 991 biological replicate (independent differentiations); TR = technical replicate (independent wells).  
 992

993 **Methods**

994 **Human pluripotent stem cell (hPSC) lines cohort and derivation**

995 We assembled a scaled discovery sample set through highly collaborative, multi-  
996 institutional efforts with the Stanley Center Biobank (Broad Institute), the Swedish  
997 Schizophrenia Cohort (Karolinska Institute), the Northern Finnish Intellectual Disability Cohort  
998 (NFID), Umea University, Massachusetts General Hospital (MGH), McLean Hospital, and  
999 GTEx. Human induced pluripotent stem cell (hiPSC) lines were generated from either fibroblasts  
1000 or lymphoblasts, and either reprogrammed in house (as previously described<sup>34</sup>), at the New York  
1001 Stem Cell Foundation (NYSCF) or at the Harvard Stem Cell Institute (HSCI) iPS core as listed  
1002 in Extended Data Table 1. The human embryonic stem cell (hESC) line H1 was obtained from  
1003 the Human Embryonic Stem Cell Facility of the Harvard Stem Cell Institute.

1004

1005 **hPSC culture**

1006 Human ESCs and iPSCs were maintained on plates coated with geltrex (life technologies,  
1007 A1413301) in StemFlex media (Gibco, A3349401) and passaged with accutase (Gibco, A11105).  
1008 All cell cultures were maintained at 37°C, 5% CO2.

1009

1010 **Infection of hPSCs with lentiviruses**

1011 Lentivirus particles were produced by Alstem (<http://www.alstembio.com/>). hPSCs were  
1012 seeded in a geltrex coated 12 well plate at a density of 100,000 cells/cm<sup>2</sup> in StemFlex medium  
1013 supplemented with rock inhibitor (Y27632, Stemgent 04-0012) and lentiviruses, at a MOI  
1014 (multiplicity of infection) of 2. 24 hours later, the medium was changed to StemFlex. The cells

1015 were grown until confluence, and then either maintained as stem cells, passaged, banked, or  
1016 induced with Doxycycline for neuronal differentiation.

1017

### 1018 **Neuronal differentiation**

1019 hPSCs were differentiated into cortical glutamatergic neurons as previously described<sup>34</sup>.  
1020 Our protocol differs from previous Ngn2-driven protocols<sup>33,89</sup> through inclusion of  
1021 developmental patterning alongside Ngn2 programming<sup>34</sup> (Fig.1b,c,f). This paradigm generates  
1022 post-mitotic excitatory cortical neurons that are highly homogeneous in terms of cell type<sup>34</sup>  
1023 compared to most differentiation paradigms which yield heterogeneous cell types<sup>90</sup>. At 4 days  
1024 post induction, cells are co-cultured with mouse glia to promote neuronal maturation and  
1025 synaptic connectivity<sup>91,92</sup>.

1026

### 1027 **RNA sequencing and alignment**

1028 We used triplicate wells of each line at each time point to reduce experimental variation.  
1029 Cells were harvested in RTLplus Lysis buffer (Qiagen 1053393) and stored at -80°C. To  
1030 minimize technical biases in readouts from cases and controls, we carried out the RNA  
1031 sequencing in mixed pools of both genotypes. Sequencing libraries were generated from 100 ng  
1032 of total RNA using the TruSeq RNA Sample Preparation kit (Illumina RS-122-2303) and  
1033 quantified using the Qubit fluorometer (Life Technologies) following the manufacturer's  
1034 instructions. Libraries were then pooled and sequenced by high output run on a HiSeq 2500  
1035 (Illumina). The total population RNA-seq fastq data was aligned against ENSEMBL human  
1036 reference genome (build GRCh37.p13/hg19) using STAR (v.2.5)<sup>93</sup>. Prior to genome aligning, we  
1037 used Trimmomatic (v.0.36)<sup>94</sup> to clip Illumina adapters and low-quality base-pairs from the ends

1038 of the sequence reads and removed reads with length < 36 base-pairs. The gene-wise read-counts  
1039 were generated from the aligned reads by featureCounts in Rsubread (v.1.32)<sup>95</sup> using GENCODE  
1040 GTF annotation version 19. The reads from the three experimental replicates were summed  
1041 together. The final read counts did not differ between cases and controls ( $11.0 \times 10^6$  and  $10.8 \times$   
1042  $10^6$  reads, respectively;  $p=0.68$ , two-sided t-test). The deleted cis genes accounted for 0.53 to  
1043 0.71% and 0.97 to 1.29 % of all read counts in carriers and controls, respectively.

1044 The plot in Figure 2a was generated as follow: we used normalized read counts from  
1045 DeSeq2 for a set of 18 canonical marker genes for pluripotency (SOX2, POU5F1, NANOG, and  
1046 MKI67), neuronal progenitor cells (NEUROD1, SOX2, EMX2, OTX2, HES1, MSI1, and  
1047 MKI67), and neuronal marker genes (RBFOX3, SYN1, DCX, MAP2, TUBB3, NCAM1, and  
1048 MAPT) to address the progress of neuronal differentiation in the data set. The normalized gene-  
1049 wise read counts were scaled to a standard score ( $z = \frac{x-\mu}{\sigma}$ ) so that the gene expression of the  
1050 different genes was presented as a difference from the average in units of standard deviations.  
1051 The mean z-score for each gene set was then calculated and plotted as a line plot across the three  
1052 cell stages (stem cells, NPCs, and neurons) with 95%-confidence intervals using inbuilt statistics  
1053 in ggplot2.

1054

## 1055 **Differential gene expression analysis**

1056 For differential gene expression analysis, we applied Wald's test for read counts that  
1057 were normalized for library size internally in DESeq2<sup>96</sup>. The differential expression analysis was  
1058 conducted separately for each cell stage to avoid any biases in gene variance modeling resulting  
1059 from gene expression differences in between SCs, NPCs, and neurons. The experimental batch  
1060 was included to the design formula in DESeq2 to correct for the 6 experimental batches in which

1061 the data was generated in. We used SVA package (version 3.32)<sup>97</sup> in R to search for latent  
1062 factors to remove any unwanted variation in the data. We first estimated the number of latent  
1063 factors using the leek method in num.sv function that was then used for calculating surrogate  
1064 variables with irw method and five iterations in sva function. The design model for sva included  
1065 experimental batch and deletion genotype. One latent factor was identified for the neuron data  
1066 and was included to the design formula in DESeq2 for differential expression. For Stem cells and  
1067 NPCs no latent factors were identified. The results for differential expression were obtained for  
1068 FDR adjusted p-value of < 0.05. A principal component analysis was performed for all genes  
1069 with more than 10 reads after normalizing the read counts by variance stabilizing transformation  
1070 in DESeq2. For differential expression analysis in the edited isogenic deletion cell lines we used  
1071 Limma-voom package<sup>98,99</sup> that enabled to model the non-independent experimental replicates  
1072 from each clone with the “duplicateCorrelation” function, which was included in the design  
1073 model by the block design in Limma.

1074

### 1075 **Power analysis**

1076 The power estimates were calculated using RNASeqPower<sup>100</sup> (R package version 1.18.0).  
1077 We calculated the median expression and variance in carriers and controls for all genes with one  
1078 or more reads (25,264 genes) in the pilot data sets. We assumed equal number of cases and  
1079 controls, while the coefficient of variance was calculated separately for cases and controls. The  
1080 alpha level was set to nominal significance of 0.05. For the final data set the power to detect fold  
1081 changes of >2 was calculated for each gene separately.

1082

1083

1084 **Enrichment for neurodevelopmental and constraint genes**

1085 Gene lists for neurodevelopmental disorder genes were compiled from the deciphering  
1086 developmental delay project<sup>45,46</sup>, and recent large scale exome sequencing study in autism<sup>27</sup>. We  
1087 included genes for which there was statistical overrepresentation of loss of function variants in  
1088 patients compared to controls (total 97 genes for ASD<sup>27</sup> and 93 for ID<sup>46</sup> genes). From the earlier  
1089 DDD-study<sup>45</sup> we included all “confirmed” developmental disorder genes that affect the brain.  
1090 We included only those that had “hemizygous” and “monoallelic” as the allelic requirement, and  
1091 mutation consequence defined as: “loss of function”, “cis-regulatory” or “promotor mutation”,  
1092 and “increased gene dosage” (total 158 genes). This resulted in a list of total 295 disease genes  
1093 for neurodevelopmental disorders (Table S5). P-values for the enrichment analyses were  
1094 calculated with hypergeometric test and binomial test in R. GO-term overrepresentations were  
1095 calculated with hypergeometric test implemented in GoStats v. 1.7.4<sup>101</sup> in R with gene  
1096 identifiers from org.Hs.eg.db. All p-values were calculated for overrepresentation using all  
1097 mapped genes from each experiment as the background gene universe. False discovery rate (fdr)  
1098 was used to adjust the raw p-values from the hypergeometric test for overrepresentation using  
1099 p.adjust function in R. Significance threshold for overrepresentation was set to fdr-adjusted p-  
1100 value smaller or equal to 0.05. The overrepresentation of synaptic GO terms was estimated by  
1101 Fisher exact test in the SYNGO online portal ([www.syngoportal.org](http://www.syngoportal.org)) using a custom background  
1102 gene set from the RNASeq data set.

1103

1104 **Protein-protein interaction network analysis**

1105 Previous efforts have shown that the observed distribution of the p-values from  
1106 differential expression studies could be modeled as a mixture of the distributed signal and

1107 uniformly distributed noise components<sup>102,103</sup>. In such approach, a threshold value could be  
1108 estimated for observed p-values to discriminate between the likely true signal from noise. Hence,  
1109 genes could be scored with logarithm of signal to noise ratio (log for making scores additive).  
1110 Further, using a reference functional network we can leverage gene weights on the map of  
1111 functional interactions to construct a node-weighted graph. Within this graph a search for the  
1112 most-weighted connected subgraph (MWCS) could be performed. This search returns a  
1113 functional module that has the strongest cumulative association to a trait being investigated.  
1114 Appearance of genes in MWCS is driven both by their differential expression p-value and  
1115 reference network topology. Thus, non-randomness of each gene's appearance could be  
1116 evaluated by randomly permuting p-values and creating a random reference network with  
1117 preserved node degrees. Estimates of how often a gene will be observed in MWCS by chance  
1118 provide an empiric metric of significance and could be used to prioritize genes within MWCS.  
1119 We implemented this strategy in R-package “PPItools” which provides a set of functions to  
1120 identify MWCS, describe its statistical properties and prioritize genes within it. We used the  
1121 InWebIM<sup>52</sup> direct protein-protein interactions network as a reference.

1122 For every time point a beta-uniform mixture distribution was fitted to a distribution of  
1123 observed p-values. Bonferroni adjusted significance threshold (0.05 / #Genes expressed) was  
1124 selected as a threshold to discriminate positively and negatively scoring genes. Scores were  
1125 estimated as a ratio between values of probability density function of Beta distribution at given  
1126 p-value and threshold p-value or  $(\alpha-1) \times (\log(x) - \log(x_{\text{threshold}}))$ , where  $\alpha$  is an estimated  
1127 parameter of Beta distribution. MWCSs for every time point of the experiment (iPSC, neuronal  
1128 progenitors and neuronal cells) were identified (Fig. 4g and Extended Data Fig. 8). Using  
1129 described above permutational scheme, for every module we assessed a non-randomness of

1130 presence for every gene found in the module (Table S8). After multiple hypothesis testing  
1131 correction (Bonferroni method used) several genes from each data set come up as significantly  
1132 functionally enriched (adjusted  $p < 0.05$ ). 36 out of 50 genes in the iPSC module were seen in  
1133 random MWCS with less than 5/1000 frequency.

1134 We further tested for excessive connectivity between significantly differentially  
1135 expressed genes and known neurodevelopmental disease genes. We selected 295 likely disease-  
1136 causing genes from the Deciphering developmental delay (DDD) project, and a recent, large  
1137 exome-sequencing study in autism (Table S5). Curated inflammatory bowel disease (IBD) and  
1138 Parkinson's disease (PD) risk gene lists (Table S5) were included as a negative control set in this  
1139 analysis. We estimated the number of connections between genes found in each of the disease  
1140 gene lists and a list of differentially expressed genes with FDR  $< 5\%$  normalized to the total  
1141 number of connections observed for all genes in both tested sets (disease and expression) in  
1142 reference data. The obtained result could be interpreted as a proportion of all connections that are  
1143 linking disease and differentially expressed genes. To evaluate significance, we generated  
1144 random gene sets of the same size as the disease gene sets and estimated an expected number of  
1145 connections with each set of differentially expressed genes. It is important to note that genes co-  
1146 expressed within the same tissue or cell type tend to have a greater number of connections  
1147 between them than would be expected for a random pair of genes. Hence, in generating random  
1148 gene sets we specifically selected genes at random to match the expression pattern of a disease  
1149 gene set in a given cell type (iPSC, neuronal progenitors or neurons). For every dataset, the  
1150 expression distribution was binned into deciles and every gene was assigned to an appropriate  
1151 bin using mean counts. Random gene sets were selected to match the distribution of genes into

1152 deciles for disease gene sets. Empirical p-values were adjusted for two disease gene sets tested  
1153 with Bonferroni correction.

1154 The PPItools package for finding MWCS and performing network prioritizations along  
1155 with documentation and source code to perform described analysis is available through GitHub  
1156 <https://github.com/alexloboda/PPIttools>.

1157

### 1158 **SNP heritability analysis**

1159 LD Score regression<sup>104</sup> and MAGMA<sup>60</sup> were used for evaluating common variant  
1160 associations in and near differentially expressed genes. Briefly for LD score regression, it can be  
1161 shown that under a basic polygenic model we expect the GWAS statistics for SNP  $j$  to be:

$$1162 E[\chi_j] = N \sum_c \tau_c l(j, c) + 1$$

1163 where  $N$  is the sample size,  $c$  is the index for the annotation category,  $l(j, c)$  is the LD score of SNP  
1164  $j$  with respect to category  $C_c$ , and  $\tau_c$  is the average per-SNP contribution to heritability of category  
1165  $C_c$ . That is, the  $\chi^2$  statistic of SNP  $j$  is expected to be a function of the total sample  $N$ , how much  
1166 the SNP tags each category  $C_c$  (quantified by  $l(j, c)$ , the sum of the squared correlation coefficient  
1167 of SNP  $j$  with each other SNP in a 1 cM window that is annotated as part of category  $C_c$ ) and  $\tau_c$ ,  
1168 the effect size of the tagged SNPs.

1169 With this model, LD Score regression allows estimation of each  $\tau_c$ . Each  $\tau_c$  is the  
1170 contribution of category  $C_c$  after controlling for all other categories in the model (we included 74  
1171 annotations that capture different genomic properties including conservation, epigenetic markers,  
1172 coding regions and LD structure similar to<sup>105</sup> and can be interpreted similarly to a coefficient  
1173 from a linear regression. Testing for significance of  $\tau_c$  is useful because it indicates whether the  
1174 per-SNP contribution to heritability of category  $C_c$  is significant after accounting for all the other

1175 annotations in the model. In addition to considering the conditional contribution of category  $C_c$   
1176 with  $c$ , the total marginal heritability explained by SNPs in category  $C_c$ , denoted  $hg2(C_c)$ , is  
1177 given by

1178

$$\hat{h}^2(C_c) = \sum_{c:j \in C_c} , \sum_{\acute{c}:j \in C_{\acute{c}}} \hat{\tau}_c$$

1179 In other words, the heritability in category  $C_c$  is the sum of the average per-SNP  
1180 heritability for all SNPs in  $C_c$ , including contributions to per-SNP heritability from other  
1181 annotations  $c'$  that overlap with category  $C_c$  (as indicated by terms of the inner sum where  $c' \neq c$ ).  
1182 Importantly,  $\hat{h}_g(C_c)$  does not depend on the categories chosen to be in the model and provides an  
1183 easier interpretation. Therefore, this quantity is the main focus of the analysis.

1184 Here we focus on  $\hat{h}_g(C_c)$  where  $C_c$  comprises HapMap SNPs 100 kb upstream and  
1185 downstream of each gene differentially expressed gene.  $\hat{h}_g(C_c)$  was calculated for three sets of  
1186 differentially expressed genes using two p-value thresholds (FDR < 5% and p < 0.05). Genes  
1187 surpassing p < 0.05 cut-off were further divided to up and down-regulated genes. Heritability  
1188 estimates were calculated for 6 sets of summary statistics from large GWAS of educational  
1189 attainment<sup>54</sup> and 5 psychiatric/neurodevelopmental disorders: ADHD<sup>55</sup>, autism spectrum  
1190 disorder<sup>56</sup>, bipolar disorder<sup>57</sup>, major depressive disorder<sup>58</sup> and schizophrenia<sup>59</sup> OR<sup>32</sup>. In addition,  
1191 the  $\hat{h}_g(C_c)$  was calculated for the up-regulated genes in neurons (p-value < 0.05) and summary  
1192 statistics for 650 phenotypes from the UK-biobank that have a significant heritability, defined by  
1193 having a heritability p-value < 0.05 after Bonferroni correction for multiple testing  
1194 (<https://www.nealelab.is/uk-biobank/>).

1195 Similar to what was done for LD-score regression we considered gene-lists of  
1196 differentially expressed genes to ask whether the differentially expressed genes are more strongly

1197 associated with each of the six phenotypes. We then used competitive gene set enrichment  
1198 analysis using gene-wise p-values<sup>56</sup> that were calculated for each trait in MAGMA v 1.06 with  
1199 standard settings<sup>60</sup>. All the results are adjusted for a set of baseline set of covariates with the goal  
1200 to minimize bias due to gene-specific characteristics: gene size, log(gene size), SNP density,  
1201 log(SNP density), inverse of the minor allele count, log(inverse of minor allele count) and  
1202 number of exons in the gene. Gene-wise p-values were calculated by gene analysis in MAGMA  
1203 and were used to identify genes underlying the stronger association signal among the upregulated  
1204 genes in neurons. LD-score regression and MAGMA competitive gene set enrichment analyses  
1205 were repeated for schizophrenia with 100 random genes lists that were matched with expression  
1206 ( $\pm 10\%$ ) to that of genes that were upregulated in deletion carriers in neurons.

1207

#### 1208 **Analysis of enrichment of differentially expressed genes in whole-exome sequencing data**

1209 We investigated if up- and down-regulated genes in 22q11.2 deletion carriers are  
1210 significantly disrupted by ultra-rare coding variants (URVs) in the whole-exomes of  
1211 schizophrenia cases and controls (previously described<sup>63,64</sup>). In the cohorts separately, we  
1212 regressed case status on the number of damaging URVs in the gene set of interest while  
1213 controlling for the total number of URVs, sex, and the first five principal components. We define  
1214 damaging URVs as putatively protein-truncating variants (stop-gain, frameshift, and splice-  
1215 donor and acceptor variants), and damaging missense variants as variants with a MPC score of  
1216  $\geq 2$ , as previously described<sup>106</sup>. We applied inverse-weighted meta-analysis to combine the test-  
1217 statistics from both studies to get a single joint P-value. We tested for enrichment in up- and  
1218 down-regulated genes, and a collection of randomly sampled neuronally-expressed genes.

1219

1220 **Motif enrichment analysis**

1221 The motif enrichment analysis was carried out by Homer software for genes whose  
1222 transcripts were found upregulated ( $\log_2$  Fold change  $> 0$ ) at day 28 neurons and p-value below  $<$   
1223 0.05. We performed a *de novo* motif analysis for human motifs using findMotifs.pl with len =  
1224 10. We curated the obtained results by setting a stringent p-value threshold ( $p < 10^{-10}$ ), visually  
1225 inspecting that observed motifs do not match only from the edges, excluded repeat sequences,  
1226 and required that the motif had a frequency of above 5%.

1227

1228 **CRISPR generation of isogenic 22q11.2 cell lines**

1229 To generate an isogenic 22q11.2 line in H1 hESCs, oligonucleotides (IDT) targeting LCR  
1230 A (ACACTGGGCACATTATAGGG) and LCR D (CATTCATCTGTCCACCCACG) were  
1231 cloned into a pU6-sgRNA vector generate sgRNA plasmids pPN298 and pPN306, respectively,  
1232 via procedures described previously <sup>107</sup>. For transfection, cells were pre-incubated with “1:1  
1233 medium” composed of a 1:1 mixture of mTeSR1 medium and “hPSC medium” [hPSC medium:  
1234 KO DMEM (Gibco 10829-018) with 20% KOSR (Gibco 10828-028), 1% Glutamax (Gibco  
1235 35050-061), 1% NEAA (Corning 25-025-Cl), 0.1% 2-mercaptoethanol (Gibco 21985-023) and  
1236 20ng/ml bFGF (EMD Millipore GF0003AF) supplemented with 10 $\mu$ M ROCK inhibitor (Y-  
1237 27632). 7  $\mu$ g Cas9 nuclease plasmid (pX459, Addgene #62988) 1.4  $\mu$ g pPN298 and 1.4  $\mu$ g  
1238 pPN306 were electroporated into 2.5x10<sup>6</sup> cells at 1050V, 30ms, 2 pulses (NEON, Life  
1239 Technologies MPK10096), as described <sup>108</sup>. Individual hPSC colonies were selected with  
1240 puromycin treatment and seeded into Geltrex-coated 96-well plates, expanded for 1-2 weeks and  
1241 duplicated for cell freezing and gDNA extraction. Clones were frozen in 96-well plates using  
1242 50% 1:1 medium plus 10 $\mu$ M Y-27632, 40%  $\neg$ FBS (VWR SH30070.03) and 10% DMSO (Sigma

1243 D2650). gDNA was extracted overnight at 55°C in Tail Lysis Buffer (Viagen 102-T) with  
1244 Proteinase K (Roche 03115828001) followed by a 1hr 90°C incubation. Droplet digital PCR  
1245 (ddPCR) was performed to determine for copy numbers of the HIRA and ZNF74 genes using  
1246 probes previously described<sup>109</sup>. SNP genotyping was performed using the Illumina Infinium  
1247 PsychArray-24 Kit on the lines to confirm the microdeletion (Broad Institute, Cambridge, MA).  
1248 Differential expression for the isogenic lines was performed by DESeq2. The results from  
1249 isogenic lines were compared to the results obtained from the discovery sample. The overlap  
1250 between the direction of fold-changes in isogenic samples were tested using binomial test for all  
1251 genes that were differentially expressed in the discovery sample. The expected probability for  
1252 overlap was calculated from all genes and was on average 0.5. The differences in gene  
1253 expression were tested by Mann-Whitney test including all genes with nominally significant p-  
1254 value in differential expression in the isogenic lines.

1255

## 1256 **DNA FISH analysis**

1257 FISH (Fluorescent In-Situ Hybridization) analysis was conducted in the isogenic control  
1258 and 22q11.2 deletion lines to analyze the copy number of the 22q11.2 region and validate the  
1259 isogenic deletion. We generated the probe using a bacterial artificial chromosome (BAC)  
1260 located in the 22q11.2 region, CTD-2300P14 (Thermo Fisher Scientific, Supplier Item: 96012),  
1261 labeled with Cy3 dUTPs (GE healthcare: PA53022), by means of nick translation (Abbott: 32-  
1262 801300), and visualized the labeled cells using confocal microscopy.

1263

1264

1265

1266 **Multielectrode Arrays (MEA)**

1267 MEA experiments and analysis were performed exactly as previously described<sup>34</sup>.  
1268 Briefly, neuronal progenitors (at day 4) were seeded on 8x8 MEA grids, each with 64  
1269 microelectrodes, in the absence or presence of mouse glia, and routinely sampled these for 42  
1270 days after Ngn2 induction and dual SMAD and WNT inhibition. Each MEA plate contained  
1271 wells from both deletion carrier and control neurons to minimize technical biases. Extracellular  
1272 spikes (action potentials) were acquired using Axion Biosystems multi-well MEA plate system  
1273 (The Maestro, Axion Biosystems; 64 electrodes per culture well). During the recording period,  
1274 the plate temperature was maintained at  $37 \pm 0.1$  °C, environmental gas composition was not  
1275 maintained outside of the incubator. Unless otherwise stated, descriptive statistics for MEA  
1276 data is presented as Tukey style box plots, showing the 1st, 2nd, and 3rd quantile (Q1, Q2,  
1277 & Q3 respectively; inter-quartile range, IQR = Q3- Q1). Box plot whiskers extend to the  
1278 most extreme data points between  $Q1-1.5*IQR$  and  $Q3+1.5*IQR$ <sup>110-112</sup>. All data points  
1279 outside the whiskers are plotted. Non-parametric 95 % confidence intervals for M are  
1280 calculated using fractional order statistics<sup>113</sup>.

1281

1282 **TMT-processing workflow**

1283 Cell pellets were lysed and 50ug protein per TMT channel were subjected to disulfide bond  
1284 reduction and alkylation. Methanol-chloroform precipitation was performed prior to protease  
1285 digestion with LysC/trypsin. Obtained peptides were labeled with the respective TMT reagents  
1286 and pooled. Enhanced proteome coverage was achieved by high-pH reversed phase fractionation  
1287 to reduce sample complexity. Peptide fractions were analyzed on an Orbitrap Fusion mass  
1288 spectrometer using SPS-MS<sup>114</sup>. Mass spectra were processed using a Sequest-based in-house  
1289 software pipeline. Peptide and protein identifications were obtained following database searching

1290 against all entries from the human UniProt database. For TMT-based reporter ion quantitation, we  
1291 extracted the summed signal-to-noise (S:N) ratio for each TMT channel. For protein-level  
1292 comparisons, peptide-spectrum-matches (PSM) were identified, quantified, and collapsed to a 1%  
1293 peptide false discovery rate (FDR) and then collapsed further to a final protein-level FDR of 1%.  
1294 Moreover, protein assembly was guided by principles of parsimony to produce the smallest set of  
1295 proteins necessary to account for all observed peptides. Proteins were quantified by summing  
1296 reporter ion counts across all matching PSMs using in-house software. Protein quantification  
1297 values were exported for further analysis.

1298

## 1299 **Analysis of protein abundances**

1300 Differences in protein abundances between deletion carriers and controls were estimated  
1301 in day 28 neurons derived from two patient (SCBB1962 and SCBB-1825) and two control lines  
1302 (SCBB1828, SCBB1827) in total 18 replicates. The abundances for the detected 8811 gene  
1303 products were  $\log_2+1$  transformed and quantile normalized in Limma package<sup>99</sup> (v. 3.3.49) in R.  
1304 A linear model including instrument run and deletion status was used to analyze differences in  
1305 the normalized protein abundances between deletion carriers and controls in Limma. The  
1306 correlation of the non-independent experimental replicates was estimated with  
1307 “duplicateCorrelation” function (average estimated inter replicate correlation was 0.83) and was  
1308 taken into account in the design model using block design in Limma. Overlap of gene products  
1309 between RNA sequence data and proteomics data (total 8585 gene products detected by both  
1310 methods) was compared using p-value<0.05 threshold. The overlap of direction of effect was  
1311 estimated with binomial test with expected probability of 0.5. The density coloring was  
1312 calculated from Kernel density estimation using densCols in R.

1313 **Immunohistochemistry**

1314 Cultured induced neurons were fixed in 4% paraformaldehyde + 20% sucrose in DPBS for 20  
1315 min at room temperature. Cells were incubated with blocking buffer containing 4% horse serum,  
1316 0.1M Glycine, and 0.3% Triton-X in PBS for 1 hour at room temperature. Primary antibodies,  
1317 diluted in 4% horse serum in PBS, were incubated overnight at 4oC. Secondary antibodies were  
1318 diluted in 4% horse serum and applied for 1 hour at room temperature. Samples were washed 3x  
1319 with PBS and imaged on spinning disc confocal microscope (Andor Dragonfly) with a 20x air  
1320 objective. The following antibodies were used: rabbit anti-SV2A (1:1000, Abcam ab32942),  
1321 chicken anti-MAP2 (1:10,000, Abcam ab5392), rabbit anti-Synaptotagmin-11 (1:1000, Synaptic  
1322 Systems 270 003). Alexafluor plus-555 and Alexafluor plus-488 conjugated secondary  
1323 antibodies (1:5,000) were obtained from Invitrogen.

1324

1325 **Image acquisition and analysis**

1326 Fluorescent images were acquired on spinning disc confocal microscope (Andor Dragonfly) at  
1327 room temperature using 20x air interface objective using Fusion software. For quantification at  
1328 least four 1024x1024 pixel fields of view from 2 different wells were taken for each line. The  
1329 images were analyzed using ImageJ software.

1330

1331 **Immunoblotting**

1332 For collection, neurons grown on glia were washed with DPBS and lysed with RIPA buffer and  
1333 1x protease inhibitor cocktail. Lysates were boiled, sonicated and centrifuged at 16,000xg for 5  
1334 minutes. The soluble fraction was separated on SDS-PAGE using Bolt system (Novex). The  
1335 proteins were transferred onto nitrocellulose membrane using iBlot2 Gel Transfer Device and

1336 immunostained using Neurexin-1 antibody (Millipore ABN161-I) and Tuj1 (Biolegend 801201)  
1337 and detected via HRP-conjugated secondary antibodies on the Chemidoc system.

1338

### 1339 **qPCR analysis**

1340 RNA isolation was performed with the Direct-Zol RNA miniprep kit (ZYMO: cat# R2051)  
1341 according to the manufacturer's instructions. To prevent DNA contamination, RNA was treated  
1342 with DNase I (ZYMO: cat# R2051). The yield of RNA was determined with a Denovix DS-11  
1343 Series Spectrophotometer (Denovix). 200ng of RNA was reverse-transcribed with the iScript  
1344 cDNA Synthesis Kit (Bio-Rad, cat# 1708890). For all analyses, RT-qPCR was carried out with  
1345 iQ SYBR Green Supermix (Bio-Rad, cat# 1708880) and specific primers for each gene  
1346 (Supplementary Table) with a CFX384 Touch Real-Time PCR Detection System (Bio-Rad).  
1347 Target genes were normalized to the geometric mean of control genes, RPL10 and GAPDH, and  
1348 relative expression compared to the mean Ct values for control and wild-type isogenic samples,  
1349 respectively.

1350 The following primers were used:

1351 MEF2C_forward	5'-CTGGTGTAACACATCGACCTC-3'
1352 MEF2C_reverse	5'-GATTGCCATACCGTCCCT-3'
1353 TBX1_forward	5'-ACGACAACGGCACATTATTC-3'
1354 TBX1_reverse	5'-CCTCGGCATATTCTCGCTATCT-3'
1355 RPL10_forward	5'-GCCGTACCCAAAGTCTCGC-3'
1356 RPL10_reverse	5'-CACAAAGCGGAAACTCATCCA-3'
1357 GAPDH_forward	5'-GGAGCGAGATCCCTCCAAAAT-3'
1358 GAPDH_reverse	5'-GGCTGTTGTCATACTTCTCATGG-3'

1359 **References**

1360

1361 1 Edelmann, L., Pandita, R. K. & Morrow, B. E. Low-copy repeats mediate the common 3-  
1362 Mb deletion in patients with velo-cardio-facial syndrome. *Am J Hum Genet* **64**, 1076-1086  
1363 (1999).

1364 2 Hoeffding, L. K. *et al.* Risk of Psychiatric Disorders Among Individuals With the 22q11.2  
1365 Deletion or Duplication: A Danish Nationwide, Register-Based Study. *JAMA Psychiatry* **74**,  
1366 282-290, doi:10.1001/jamapsychiatry.2016.3939 (2017).

1367 3 Swillen, A. & McDonald-McGinn, D. Developmental trajectories in 22q11.2 deletion. *Am J  
1368 Med Genet C Semin Med Genet* **169**, 172-181, doi:10.1002/ajmg.c.31435 (2015).

1369 4 Horowitz, A., Shifman, S., Rivlin, N., Pisante, A. & Darvasi, A. A survey of the 22q11  
1370 microdeletion in a large cohort of schizophrenia patients. *Schizophr Res* **73**, 263-267,  
1371 doi:10.1016/j.schres.2004.02.008 (2005).

1372 5 Kates, W. R. *et al.* Neurocognitive and familial moderators of psychiatric risk in  
1373 velocardiofacial (22q11.2 deletion) syndrome: a longitudinal study. *Psychol Med* **45**, 1629-  
1374 1639, doi:10.1017/S0033291714002724 (2015).

1375 6 Monks, S. *et al.* Further evidence for high rates of schizophrenia in 22q11.2 deletion  
1376 syndrome. *Schizophr Res* **153**, 231-236, doi:10.1016/j.schres.2014.01.020 (2014).

1377 7 Schneider, M. *et al.* Psychiatric disorders from childhood to adulthood in 22q11.2 deletion  
1378 syndrome: results from the International Consortium on Brain and Behavior in 22q11.2  
1379 Deletion Syndrome. *Am J Psychiatry* **171**, 627-639, doi:10.1176/appi.ajp.2013.13070864  
1380 (2014).

1381 8 Marshall, C. R. *et al.* Contribution of copy number variants to schizophrenia from a  
1382 genome-wide study of 41,321 subjects. *Nat Genet* **49**, 27-35, doi:10.1038/ng.3725 (2017).

1383 9 Costales, J. L. & Kolevzon, A. Phelan-McDermid Syndrome and SHANK3: Implications for  
1384 Treatment. *Neurotherapeutics* **12**, 620-630, doi:10.1007/s13311-015-0352-z (2015).

1385 10 Devaraju, P. *et al.* Haploinsufficiency of the 22q11.2 microdeletion gene Mrpl40 disrupts  
1386 short-term synaptic plasticity and working memory through dysregulation of  
1387 mitochondrial calcium. *Mol Psychiatry* **22**, 1313-1326, doi:10.1038/mp.2016.75 (2017).

1388 11 Devaraju, P. & Zakharenko, S. S. Mitochondria in complex psychiatric disorders: Lessons  
1389 from mouse models of 22q11.2 deletion syndrome: Hemizygous deletion of several  
1390 mitochondrial genes in the 22q11.2 genomic region can lead to symptoms associated with  
1391 neuropsychiatric disease. *Bioessays* **39**, doi:10.1002/bies.201600177 (2017).

1392 12 Diamantopoulou, A. *et al.* Loss-of-function mutation in Mirta22/Emc10 rescues specific  
1393 schizophrenia-related phenotypes in a mouse model of the 22q11.2 deletion. *Proc Natl  
1394 Acad Sci U S A* **114**, E6127-E6136, doi:10.1073/pnas.1615719114 (2017).

1395 13 Fenelon, K. *et al.* Deficiency of Dgcr8, a gene disrupted by the 22q11.2 microdeletion,  
1396 results in altered short-term plasticity in the prefrontal cortex. *Proc Natl Acad Sci U S A*  
1397 **108**, 4447-4452, doi:10.1073/pnas.1101219108 (2011).

1398 14 Hsu, R. *et al.* Nogo Receptor 1 (RTN4R) as a candidate gene for schizophrenia: analysis  
1399 using human and mouse genetic approaches. *PLoS One* **2**, e1234,  
1400 doi:10.1371/journal.pone.0001234 (2007).

1401 15 Karayiorgou, M. & Gogos, J. A. The molecular genetics of the 22q11-associated  
1402 schizophrenia. *Brain Res Mol Brain Res* **132**, 95-104,  
1403 doi:10.1016/j.molbrainres.2004.09.029 (2004).

1404 16 Kimura, H. *et al.* A novel rare variant R292H in RTN4R affects growth cone formation and  
1405 possibly contributes to schizophrenia susceptibility. *Transl Psychiatry* **7**, e1214,  
1406 doi:10.1038/tp.2017.170 (2017).

1407 17 Meechan, D. W., Maynard, T. M., Tucker, E. S. & LaMantia, A. S. Three phases of  
1408 DiGeorge/22q11 deletion syndrome pathogenesis during brain development: patterning,  
1409 proliferation, and mitochondrial functions of 22q11 genes. *Int J Dev Neurosci* **29**, 283-294,  
1410 doi:10.1016/j.ijdevneu.2010.08.005 (2011).

1411 18 Mukai, J. *et al.* Evidence that the gene encoding ZDHHC8 contributes to the risk of  
1412 schizophrenia. *Nat Genet* **36**, 725-731, doi:10.1038/ng1375 (2004).

1413 19 Paronett, E. M., Meechan, D. W., Karpinski, B. A., LaMantia, A. S. & Maynard, T. M.  
1414 Ranbp1, Deleted in DiGeorge/22q11.2 Deletion Syndrome, is a Microcephaly Gene That  
1415 Selectively Disrupts Layer 2/3 Cortical Projection Neuron Generation. *Cereb Cortex* **25**,  
1416 3977-3993, doi:10.1093/cercor/bhu285 (2015).

1417 20 Stark, K. L. *et al.* Altered brain microRNA biogenesis contributes to phenotypic deficits in  
1418 a 22q11-deletion mouse model. *Nat Genet* **40**, 751-760, doi:10.1038/ng.138 (2008).

1419 21 Wang, X., Bryan, C., LaMantia, A. S. & Mendelowitz, D. Altered neurobiological function  
1420 of brainstem hypoglossal neurons in DiGeorge/22q11.2 Deletion Syndrome. *Neuroscience*  
1421 **359**, 1-7, doi:10.1016/j.neuroscience.2017.06.057 (2017).

1422 22 Bassett, A. S. *et al.* Rare Genome-Wide Copy Number Variation and Expression of  
1423 Schizophrenia in 22q11.2 Deletion Syndrome. *Am J Psychiatry* **174**, 1054-1063,  
1424 doi:10.1176/appi.ajp.2017.16121417 (2017).

1425 23 Bergen, S. E. *et al.* Joint Contributions of Rare Copy Number Variants and Common SNPs  
1426 to Risk for Schizophrenia. *Am J Psychiatry*, appiajp201817040467,  
1427 doi:10.1176/appi.ajp.2018.17040467 (2018).

1428 24 Cleynen, I. *et al.* Genetic contributors to risk of schizophrenia in the presence of a 22q11.2  
1429 deletion. *Mol Psychiatry*, doi:10.1038/s41380-020-0654-3 (2020).

1430 25 Davies, R. W. *et al.* Using common genetic variation to examine phenotypic expression  
1431 and risk prediction in 22q11.2 deletion syndrome. *Nat Med* **26**, 1912-1918,  
1432 doi:10.1038/s41591-020-1103-1 (2020).

1433 26 An, J. Y. *et al.* Genome-wide de novo risk score implicates promoter variation in autism  
1434 spectrum disorder. *Science* **362**, doi:10.1126/science.aat6576 (2018).

1435 27 F. Kyle Satterstrom, J. A. K., Jiebiao Wang, Michael S. Breen, Silvia, De Rubeis, J.-Y. A.,  
1436 Minshi Peng, Ryan Collins, Jakob Grove, Lambertus & Klei, C. S., et al and, Bernie Devlin, #,  
1437 Stephan J. Sanders#, Kathryn Roeder#, Joseph D. Buxbaum, Mark J. Daly. Novel genes for  
1438 autism implicate both excitatory and inhibitory cell lineages in risk. *Biorxiv* (2018).

1439 28 Sanders, S. J. *et al.* Whole genome sequencing in psychiatric disorders: the WGSPD  
1440 consortium. *Nat Neurosci* **20**, 1661-1668, doi:10.1038/s41593-017-0017-9 (2017).

1441 29 Weiner, D. J. *et al.* Polygenic transmission disequilibrium confirms that common and rare  
1442 variation act additively to create risk for autism spectrum disorders. *Nat Genet* **49**, 978-  
1443 985, doi:10.1038/ng.3863 (2017).

1444 30 Finucane, H. K. *et al.* Heritability enrichment of specifically expressed genes identifies  
1445 disease-relevant tissues and cell types. *Nat Genet* **50**, 621-629, doi:10.1038/s41588-018-  
1446 0081-4 (2018).

1447 31 Koopmans, F. *et al.* SynGO: An Evidence-Based, Expert-Curated Knowledge Base for the  
1448 Synapse. *Neuron* **103**, 217-234 e214, doi:10.1016/j.neuron.2019.05.002 (2019).

1449 32 Schizophrenia Working Group of the Psychiatric Genomics, C. Biological insights from 108  
1450 schizophrenia-associated genetic loci. *Nature* **511**, 421-427, doi:10.1038/nature13595  
1451 (2014).

1452 33 Zhang, Y. *et al.* Rapid single-step induction of functional neurons from human pluripotent  
1453 stem cells. *Neuron* **78**, 785-798, doi:10.1016/j.neuron.2013.05.029 (2013).

1454 34 Nehme, R. *et al.* Combining NGN2 Programming with Developmental Patterning  
1455 Generates Human Excitatory Neurons with NMDAR-Mediated Synaptic Transmission. *Cell*  
1456 *Rep* **23**, 2509-2523, doi:10.1016/j.celrep.2018.04.066 (2018).

1457 35 Fan, L. Z. *et al.* All-optical synaptic electrophysiology probes mechanism of ketamine-  
1458 induced disinhibition. *Nat Methods* **15**, 823-831, doi:10.1038/s41592-018-0142-8 (2018).

1459 36 Mitchell JM, N. J., Ghosh S, Handsaker RE, Mello CJ, Meyer D, Raghunathan K, de Rivera  
1460 M, Tegtmeyer M, Hawes D, Neumann A, Nehme R, Eggan K, McCarroll SA. . Mapping  
1461 genetic effects on cellular phenotypes with “cell villages”. . *BioRxiv and Cell*, *in revision*  
1462 (2020).

1463 37 Wells M, S. M., Piccioni F, Hill E, Mitchell J, Worringer K, Raymond J, Kommineni S, Chan  
1464 K, Ho D, Peterson B, Siekmann M, Pietilainen O, Nehme R, Kaykas A, Eggan K. . Genome-  
1465 wide screens in accelerated human stem cellderived neural progenitor cells identify Zika  
1466 virus host factors and drivers of proliferation *BioRxiv* (2018).

1467 38 Biswas, A. B. & Furniss, F. Cognitive phenotype and psychiatric disorder in 22q11.2  
1468 deletion syndrome: A review. *Res Dev Disabil* **53-54**, 242-257,  
1469 doi:10.1016/j.ridd.2016.02.010 (2016).

1470 39 Fiksinski, A. M. *et al.* Autism Spectrum and psychosis risk in the 22q11.2 deletion  
1471 syndrome. Findings from a prospective longitudinal study. *Schizophr Res* **188**, 59-62,  
1472 doi:10.1016/j.schres.2017.01.032 (2017).

1473 40 Lin, M. *et al.* Integrative transcriptome network analysis of iPSC-derived neurons from  
1474 schizophrenia and schizoaffective disorder patients with 22q11.2 deletion. *BMC Syst Biol*  
1475 **10**, 105, doi:10.1186/s12918-016-0366-0 (2016).

1476 41 Khan, T. A. *et al.* Neuronal defects in a human cellular model of 22q11.2 deletion  
1477 syndrome. *Nat Med*, doi:10.1038/s41591-020-1043-9 (2020).

1478 42 Lek, M. *et al.* Analysis of protein-coding genetic variation in 60,706 humans. *Nature* **536**,  
1479 285-291, doi:10.1038/nature19057 (2016).

1480 43 McDonald-McGinn, D. M. *et al.* 22q11.2 deletion syndrome. *Nat Rev Dis Primers* **1**, 15071,  
1481 doi:10.1038/nrdp.2015.71 (2015).

1482 44 Dantas, A. G. *et al.* Downregulation of genes outside the deleted region in individuals with  
1483 22q11.2 deletion syndrome. *Hum Genet* **138**, 93-103, doi:10.1007/s00439-018-01967-6  
1484 (2019).

1485 45 Deciphering Developmental Disorders, S. Large-scale discovery of novel genetic causes of  
1486 developmental disorders. *Nature* **519**, 223-228, doi:10.1038/nature14135 (2015).

1487 46 Deciphering Developmental Disorders, S. Prevalence and architecture of de novo  
1488 mutations in developmental disorders. *Nature* **542**, 433-438, doi:10.1038/nature21062  
1489 (2017).

1490 47 The Schizophrenia Working Group of the Psychiatric Genomics Consortium, S. R., James  
1491 TR Walters, Michael C O'Donovan. Mapping genomic loci prioritises genes and implicates  
1492 synaptic biology in schizophrenia. *medRxiv*,  
1493 doi:<https://doi.org/10.1101/2020.09.12.20192922> (2020).

1494 48 Yap, E. L. & Greenberg, M. E. Activity-Regulated Transcription: Bridging the Gap between  
1495 Neural Activity and Behavior. *Neuron* **100**, 330-348, doi:10.1016/j.neuron.2018.10.013  
1496 (2018).

1497 49 Pane, L. S. *et al.* Tbx1 represses Mef2c gene expression and is correlated with histone 3  
1498 deacetylation of the anterior heart field enhancer. *Dis Model Mech* **11**,  
1499 doi:10.1242/dmm.029967 (2018).

1500 50 Pane, L. S. *et al.* Tbx1 is a negative modulator of Mef2c. *Hum Mol Genet* **21**, 2485-2496,  
1501 doi:10.1093/hmg/dds063 (2012).

1502 51 Rossin, E. J. *et al.* Proteins encoded in genomic regions associated with immune-mediated  
1503 disease physically interact and suggest underlying biology. *PLoS Genet* **7**, e1001273,  
1504 doi:10.1371/journal.pgen.1001273 (2011).

1505 52 Li, T. *et al.* A scored human protein-protein interaction network to catalyze genomic  
1506 interpretation. *Nat Methods* **14**, 61-64, doi:10.1038/nmeth.4083 (2017).

1507 53 Satterstrom, F. K. *et al.* Large-Scale Exome Sequencing Study Implicates Both  
1508 Developmental and Functional Changes in the Neurobiology of Autism. *Cell* **180**, 568-584  
1509 e523, doi:10.1016/j.cell.2019.12.036 (2020).

1510 54 Lee, J. J. *et al.* Gene discovery and polygenic prediction from a genome-wide association  
1511 study of educational attainment in 1.1 million individuals. *Nat Genet* **50**, 1112-1121,  
1512 doi:10.1038/s41588-018-0147-3 (2018).

1513 55 Demontis, D. *et al.* Discovery of the first genome-wide significant risk loci for attention  
1514 deficit/hyperactivity disorder. *Nat Genet* **51**, 63-75, doi:10.1038/s41588-018-0269-7  
1515 (2019).

1516 56 Grove, J. *et al.* Identification of common genetic risk variants for autism spectrum  
1517 disorder. *Nat Genet* **51**, 431-444, doi:10.1038/s41588-019-0344-8 (2019).

1518 57 Psychiatric, G. C. B. D. W. G. Large-scale genome-wide association analysis of bipolar  
1519 disorder identifies a new susceptibility locus near ODZ4. *Nat Genet* **43**, 977-983,  
1520 doi:10.1038/ng.943 (2011).

1521 58 Wray, N. R. *et al.* Genome-wide association analyses identify 44 risk variants and refine  
1522 the genetic architecture of major depression. *Nat Genet* **50**, 668-681,  
1523 doi:10.1038/s41588-018-0090-3 (2018).

1524 59 Pardinas, A. F. *et al.* Common schizophrenia alleles are enriched in mutation-intolerant  
1525 genes and in regions under strong background selection. *Nat Genet* **50**, 381-389,  
1526 doi:10.1038/s41588-018-0059-2 (2018).

1527 60 de Leeuw, C. A., Mooij, J. M., Heskes, T. & Posthuma, D. MAGMA: generalized gene-set  
1528 analysis of GWAS data. *PLoS Comput Biol* **11**, e1004219,  
1529 doi:10.1371/journal.pcbi.1004219 (2015).

1530 61 Purcell, S. M. *et al.* A polygenic burden of rare disruptive mutations in schizophrenia.  
1531 62 *Nature* **506**, 185-190, doi:10.1038/nature12975 (2014).

1532 62 Fromer, M. *et al.* De novo mutations in schizophrenia implicate synaptic networks. *Nature*  
1533 63 **506**, 179-184, doi:10.1038/nature12929 (2014).

1534 63 Genovese, G. *et al.* Increased burden of ultra-rare protein-altering variants among 4,877  
1535 64 individuals with schizophrenia. *Nat Neurosci* **19**, 1433-1441, doi:10.1038/nn.4402 (2016).

1536 64 Singh, T. *et al.* The contribution of rare variants to risk of schizophrenia in individuals with  
1537 65 and without intellectual disability. *Nat Genet* **49**, 1167-1173, doi:10.1038/ng.3903 (2017).

1538 65 Singh T, P. T., Curtis D, Akil H, Eissa MA, Barchas JD, Bass N, Bigdely TB, Breen G, Bromet  
1539 66 EJ, Buckley PF, Bunney WE, Bybjerg-Grauholt J, Byerley WF, Chapman SB, Chen WJ,  
1540 67 Churchhouse C, Craddock N, Curtis C, Cusick C, DeLisi L, Dodge S, Escamilla MA, Eskelin  
1541 68 S, Fanous AH, Faraone SV, Fiorentino A, Francioli L, Gabriel SB, Gage D, Taliun SAG, Ganna  
1542 69 A, Genovese G, Glahn DC, Grove J, Hall MH, Hamalainen E, Heyne HO, Holi M, Hougaard  
1543 70 DM, Howrigan DP, Huang H, Hwu HG, Kahn RS, Kang HM, Karczewski K, Kirov G, Knowles  
1544 71 JA, Lee FS, Lehrer DS, Lesca F, Malaspina D, Marder SR, McCarroll SA, Medeiros H, Milani  
1545 72 L, Morley CP, Morris DW, Mortensen PB, Myers RM, Nordentoft M, O'Brien NL, Olivares  
1546 73 AM, Ongur D, Ouwehand WH, Palmer DS, Paunio T, Quested D, Rapaport MH, Rees E,  
1547 74 Rollins B, Satterstrom FK, Schatzberg A, Scolnick E, Scott L, Sharp SI, Sklar P, Smoller JW,  
1548 75 Sobell JI, Solomonson M, Stevens CR, Suvisaari J, Tiao G, Watson SJ, Watts NA, Blackwood  
1549 76 DH, Borglum A, Cohen BM, Corvin AP, Esko T, Freimer NB, Glatt SJ, Hultman CM, McQuillin  
1550 77 A, Palotie A, Pato CN, Pato MT, Pulver AE, Clair DS, Tsuang MT, Vawter MP, Walters JT,  
1551 78 Werge T, Ophoff RA, Sullivan PF, Owen MJ, Boehnke M, O'Donovan M, Neale BM, Daly  
1552 79 MJ. Exome sequencing identifies rare coding variants in 10 genes which confer substantial  
1553 80 risk for schizophrenia. *Medrxiv*, doi:medRxiv 2020.09.18.20192815; doi:  
1554 81 <https://doi.org/10.1101/2020.09.18.20192815> (2020).

1555 66 Flavell, S. W. *et al.* Activity-dependent regulation of MEF2 transcription factors suppresses  
1556 67 excitatory synapse number. *Science* **311**, 1008-1012, doi:10.1126/science.1122511  
1557 68 (2006).

1558 67 Flavell, S. W. *et al.* Genome-wide analysis of MEF2 transcriptional program reveals  
1559 69 synaptic target genes and neuronal activity-dependent polyadenylation site selection.  
1560 70 *Neuron* **60**, 1022-1038, doi:10.1016/j.neuron.2008.11.029 (2008).

1561 68 Becher, A. *et al.* The synaptophysin-synaptobrevin complex: a hallmark of synaptic vesicle  
1562 69 maturation. *J Neurosci* **19**, 1922-1931 (1999).

1563 69 Chang, W. P. & Sudhof, T. C. SV2 renders primed synaptic vesicles competent for Ca<sup>2+</sup> -  
1564 70 induced exocytosis. *J Neurosci* **29**, 883-897, doi:10.1523/JNEUROSCI.4521-08.2009  
1565 71 (2009).

1566 70 Mattheisen, M. *et al.* Genetic variation at the synaptic vesicle gene SV2A is associated  
1567 71 with schizophrenia. *Schizophr Res* **141**, 262-265, doi:10.1016/j.schres.2012.08.027  
1568 72 (2012).

1569 71 Rujescu, D. *et al.* Disruption of the neurexin 1 gene is associated with schizophrenia. *Hum*  
1570 72 *Mol Genet* **18**, 988-996, doi:10.1093/hmg/ddn351 (2009).

1571 72 Stefansson, H. *et al.* CNVs conferring risk of autism or schizophrenia affect cognition in  
1572 73 controls. *Nature* **505**, 361-366, doi:10.1038/nature12818 (2014).

1573 73 Inoue, S. *et al.* Synaptotagmin XI as a candidate gene for susceptibility to schizophrenia.  
1574 *Am J Med Genet B Neuropsychiatr Genet* **144B**, 332-340, doi:10.1002/ajmg.b.30465  
1575 (2007).

1576 74 Lelieveld, S. H. *et al.* Meta-analysis of 2,104 trios provides support for 10 new genes for  
1577 intellectual disability. *Nat Neurosci* **19**, 1194-1196, doi:10.1038/nn.4352 (2016).

1578 75 Finnema, S. J. *et al.* Imaging synaptic density in the living human brain. *Sci Transl Med* **8**,  
1579 348ra396, doi:10.1126/scitranslmed.aaf6667 (2016).

1580 76 Onwordi, E. C. *et al.* Synaptic density marker SV2A is reduced in schizophrenia patients  
1581 and unaffected by antipsychotics in rats. *Nat Commun* **11**, 246, doi:10.1038/s41467-019-  
1582 14122-0 (2020).

1583 77 Araujo, D. J. *et al.* FoxP1 orchestration of ASD-relevant signaling pathways in the striatum.  
1584 *Genes Dev* **29**, 2081-2096, doi:10.1101/gad.267989.115 (2015).

1585 78 Sugathan, A. *et al.* CHD8 regulates neurodevelopmental pathways associated with autism  
1586 spectrum disorder in neural progenitors. *Proc Natl Acad Sci U S A* **111**, E4468-4477,  
1587 doi:10.1073/pnas.1405266111 (2014).

1588 79 Li, M. *et al.* Integrative functional genomic analysis of human brain development and  
1589 neuropsychiatric risks. *Science* **362**, doi:10.1126/science.aat7615 (2018).

1590 80 Forsyth, J. K. *et al.* Synaptic and Gene Regulatory Mechanisms in Schizophrenia, Autism,  
1591 and 22q11.2 Copy Number Variant-Mediated Risk for Neuropsychiatric Disorders. *Biol  
1592 Psychiatry* **87**, 150-163, doi:10.1016/j.biopsych.2019.06.029 (2020).

1593 81 Kahn, J. B., Port, R. G., Anderson, S. A. & Coulter, D. A. Modular, Circuit-Based  
1594 Interventions Rescue Hippocampal-Dependent Social and Spatial Memory in a 22q11.2  
1595 Deletion Syndrome Mouse Model. *Biol Psychiatry* **88**, 710-718,  
1596 doi:10.1016/j.biopsych.2020.04.028 (2020).

1597 82 Ellegood, J. *et al.* Neuroanatomical phenotypes in a mouse model of the 22q11.2  
1598 microdeletion. *Mol Psychiatry* **19**, 99-107, doi:10.1038/mp.2013.112 (2014).

1599 83 Long, J. M. *et al.* Behavior of mice with mutations in the conserved region deleted in  
1600 velocardiofacial/DiGeorge syndrome. *Neurogenetics* **7**, 247-257, doi:10.1007/s10048-  
1601 006-0054-0 (2006).

1602 84 Mukai, J. *et al.* Molecular substrates of altered axonal growth and brain connectivity in a  
1603 mouse model of schizophrenia. *Neuron* **86**, 680-695, doi:10.1016/j.neuron.2015.04.003  
1604 (2015).

1605 85 Meng, Q. *et al.* The DGCR5 long noncoding RNA may regulate expression of several  
1606 schizophrenia-related genes. *Sci Transl Med* **10**, doi:10.1126/scitranslmed.aat6912  
1607 (2018).

1608 86 Won, H. *et al.* Chromosome conformation elucidates regulatory relationships in  
1609 developing human brain. *Nature* **538**, 523-527, doi:10.1038/nature19847 (2016).

1610 87 Spielmann, M., Lupianez, D. G. & Mundlos, S. Structural variation in the 3D genome. *Nat  
1611 Rev Genet* **19**, 453-467, doi:10.1038/s41576-018-0007-0 (2018).

1612 88 Zhang, X. *et al.* Local and global chromatin interactions are altered by large genomic  
1613 deletions associated with human brain development. *Nat Commun* **9**, 5356,  
1614 doi:10.1038/s41467-018-07766-x (2018).

1615 89 Busskamp, V. *et al.* Rapid neurogenesis through transcriptional activation in human stem  
1616 cells. *Molecular systems biology* **10**, 760, doi:10.15252/msb.20145508 (2014).

1617 90 Chambers, S. M. *et al.* Highly efficient neural conversion of human ES and iPS cells by dual  
1618 inhibition of SMAD signaling. *Nat Biotechnol* **27**, 275-280, doi:10.1038/nbt.1529 (2009).  
1619 91 Eroglu, C. & Barres, B. A. Regulation of synaptic connectivity by glia. *Nature* **468**, 223-231,  
1620 doi:10.1038/nature09612 (2010).  
1621 92 Pfrieger, F. W. Roles of glial cells in synapse development. *Cellular and molecular life  
1622 sciences : CMLS* **66**, 2037-2047, doi:10.1007/s00018-009-0005-7 (2009).  
1623 93 Dobin, A. *et al.* STAR: ultrafast universal RNA-seq aligner. *Bioinformatics* **29**, 15-21,  
1624 doi:10.1093/bioinformatics/bts635 (2013).  
1625 94 Bolger, A. M., Lohse, M. & Usadel, B. Trimmomatic: a flexible trimmer for Illumina  
1626 sequence data. *Bioinformatics* **30**, 2114-2120, doi:10.1093/bioinformatics/btu170 (2014).  
1627 95 Liao, Y., Smyth, G. K. & Shi, W. featureCounts: an efficient general purpose program for  
1628 assigning sequence reads to genomic features. *Bioinformatics* **30**, 923-930,  
1629 doi:10.1093/bioinformatics/btt656 (2014).  
1630 96 Love, M. I., Huber, W. & Anders, S. Moderated estimation of fold change and dispersion  
1631 for RNA-seq data with DESeq2. *Genome Biol* **15**, 550, doi:10.1186/s13059-014-0550-8  
1632 (2014).  
1633 97 Leek, J. T., Johnson, W. E., Parker, H. S., Jaffe, A. E. & Storey, J. D. The sva package for  
1634 removing batch effects and other unwanted variation in high-throughput experiments.  
1635 *Bioinformatics* **28**, 882-883, doi:10.1093/bioinformatics/bts034 (2012).  
1636 98 Law, C. W., Chen, Y., Shi, W. & Smyth, G. K. voom: Precision weights unlock linear model  
1637 analysis tools for RNA-seq read counts. *Genome Biol* **15**, R29, doi:10.1186/gb-2014-15-2-  
1638 r29 (2014).  
1639 99 Ritchie, M. E. *et al.* limma powers differential expression analyses for RNA-sequencing  
1640 and microarray studies. *Nucleic Acids Res* **43**, e47, doi:10.1093/nar/gkv007 (2015).  
1641 100 Hart, S. N., Therneau, T. M., Zhang, Y., Poland, G. A. & Kocher, J. P. Calculating sample size  
1642 estimates for RNA sequencing data. *J Comput Biol* **20**, 970-978,  
1643 doi:10.1089/cmb.2012.0283 (2013).  
1644 101 Falcon, S. & Gentleman, R. Using G0stats to test gene lists for GO term association.  
1645 *Bioinformatics* **23**, 257-258, doi:10.1093/bioinformatics/btl567 (2007).  
1646 102 Beisser, D., Klau, G. W., Dandekar, T., Muller, T. & Dittrich, M. T. BioNet: an R-Package for  
1647 the functional analysis of biological networks. *Bioinformatics* **26**, 1129-1130,  
1648 doi:10.1093/bioinformatics/btq089 (2010).  
1649 103 Dittrich, M. T., Klau, G. W., Rosenwald, A., Dandekar, T. & Muller, T. Identifying functional  
1650 modules in protein-protein interaction networks: an integrated exact approach.  
1651 *Bioinformatics* **24**, i223-231, doi:10.1093/bioinformatics/btn161 (2008).  
1652 104 Finucane, H. K. *et al.* Partitioning heritability by functional annotation using genome-wide  
1653 association summary statistics. *Nat Genet* **47**, 1228-1235, doi:10.1038/ng.3404 (2015).  
1654 105 Gazal, S. *et al.* Linkage disequilibrium-dependent architecture of human complex traits  
1655 shows action of negative selection. *Nat Genet* **49**, 1421-1427, doi:10.1038/ng.3954  
1656 (2017).  
1657 106 Samocha KE, K. J., Karczewski KJ, O'Donnell-Luria AH, Pierce-Hoffman E, MacArthur DG,  
1658 Neale BM, Daly MJ. Regional missense constraint improves variant deleteriousness  
1659 prediction. *Biorxiv* (2017).

1660 107 Cong, L. *et al.* Multiplex genome engineering using CRISPR/Cas systems. *Science* **339**, 819-  
1661 823, doi:10.1126/science.1231143 (2013).

1662 108 Hazelbaker, D. Z. *et al.* A Scaled Framework for CRISPR Editing of Human Pluripotent Stem  
1663 Cells to Study Psychiatric Disease. *Stem Cell Reports* **9**, 1315-1327,  
1664 doi:10.1016/j.stemcr.2017.09.006 (2017).

1665 109 Hwang, V. J. *et al.* Mapping the deletion endpoints in individuals with 22q11.2 deletion  
1666 syndrome by droplet digital PCR. *BMC Med Genet* **15**, 106, doi:10.1186/s12881-014-0106-  
1667 5 (2014).

1668 110 Krzywinski, M. & Altman, N. Visualizing samples with box plots. *Nature methods* **11**, 119-  
1669 120 (2014).

1670 111 McGill, R., Tukey, J.W. and Larsen, W.A. . Variations of Box Plots. *The American Statistician*  
1671 **32**, 12-16 (1978).

1672 112 Streit, M. & Gehlenborg, N. Bar charts and box plots. *Nature methods* **11**, 117 (2014).

1673 113 Hutson, A. D. Calculating nonparametric confidence intervals for quantiles using fractional  
1674 order statistics. . *Journal of Applied Statistics* **26** 343-353 (1999).

1675 114 McAlister, G. C. *et al.* MultiNotch MS3 enables accurate, sensitive, and multiplexed  
1676 detection of differential expression across cancer cell line proteomes. *Anal Chem* **86**,  
1677 7150-7158, doi:10.1021/ac502040v (2014).

1678